ISTITUTO SUPERIORE DI SANITÀ

SNIFFER system: a multipurpose aerial platform for large area radiological surveillance, emergency management and air pollution monitoring

Donato Maurizio Castelluccio,
Evaristo Cisbani, Salvatore Frullani

Dipartimento di Tecnologie e Salute

ISSN 1123-3117
Rapporti ISTISAN
07/33

Istituto Superiore di Sanità
SNIFFER system: a multipurpose aerial platform for large area radiological surveillance, emergency management and air pollution monitoring.
Donato Maurizio Castelluccio, Evaristo Cisbani, Salvatore Frullani
2007, 51 p. Rapporti ISTISAN 07/33

After several years of research and development, the Istituto Superiore di Sanità (the National Institute of Health in Italy) in collaboration with the Ministry of Environment has implemented and is now commissioning the SNIFFER system, a multipurpose air sampling platform based on fixed wing aircraft. The SNIFFER consists of two air sampling lines: one is dedicated to the identification and measurement, in isokinetic condition, of the atmospheric aerosol radioactive contamination and the other one to the quantitative monitoring of organic compounds and aromatic hydrocarbons. The sampled data are combined with environmental (temperature, pressure, air density and speed) and geolocation information for a full characterization of the sampling conditions and their temporal and geographical location. Radiological surveillance, quantitative assessment (since the early phase of a radiological emergency) and air quality monitoring on large areas represent the main target applications of the SNIFFER. The present report is devoted to the description of the system: from its motivations to the main design issues and the details of its implementation.
Key words: Environmental monitoring, Radiological surveillance, Nuclear spectroscopy

Istituto Superiore di Sanità
Il sistema SNIFFER: una piattaforma aerea multi-funzione per la sorveglianza radiologica, la gestione di un'emergenza radiologica e il monitoraggio dell'inquinamento atmosferico.
Donato Maurizio Castelluccio, Evaristo Cisbani, Salvatore Frullani
2007, 51 p. Rapporti ISTISAN 07/33 (in inglese)

Dopo diversi anni di ricerca e sviluppo, l'Istituto Superire di Sanità in collaborazione con il Ministero dell'Ambiente ha realizzato e sta ora testando il sistema SNIFFER, una piattaforma multi-funzione per il campionamento dell'aria ospitata su un aereo ad ala fissa. Lo SNIFFER consiste di due linee di campionamento dell'aria: una è dedicata all'identificazione e misura, in condizioni di isocinetismo, della contaminazione radioattiva dell'atmosfera e del suolo; l'altra è rivolta al monitoraggio quantitativo di composti organici e idrocarburi aromatici. I dati campionati sono combinati ad informazioni ambientali (temperatura, pressione, densità e velocità dell'aria) e di geolocazione per una completa caratterizzazione delle condizioni di campionamento e della loro locazione temporale e geografica. Sorveglianza radiologica, valutazione quantitativa (sin dalle prime fasi di un'emergenza radiologica) e monitoraggio della qualità dell'aria su ampie superfici rappresentano le principali applicazioni dello SNIFFER. Il presente rapporto descrive il sistema a partire dalle motivazioni che l'hanno promosso, fino alle principali questioni di progetto e a dettagli della sua implementazione.
Parole chiave: Monitoraggio ambientale, Sorveglianza radiologica, Spettroscopia nucleare

Si ringraziano: Stefano Colilli, Fausto Giuliani, Rolando Fratoni, Angelo Mostarda, Luigi Pierangeli (*Dipartimento di Tecnologia e Salute, Istituto Superiore di Sanità*) e Carlo Marchiori e Gianfranco Paoloni (*Dipartimento di Ingegneria Aeronautica dell'Università La Sapienza*) per la collaborazione tecnica alla progettazione e alla realizzazione del sistema SNIFFER; Luigi Paoletti (*Dipartimento di Tecnologia e Salute, Istituto Superiore di Sanità*), Sergio Fuselli, Achille Marconi (*Dipartimento di Ambiente e Connessa Prevenzione Primaria, Istituto Superiore di Sanità*) e Salvatore Chiavarini (*ENEA, Casaccia*) per il prezioso contributo per la parte riguardante il campionamento e l'analisi dei microinquinanti organici.

Per informazioni rivolgersi a: evaristo.cisbani@iss.it; donato.castelluccio@iss.it; salvatore.frullani@iss.it

Il rapporto è disponibile online sul sito di questo Istituto: www.iss.it.

Citare questo documento come segue:
Castelluccio DM, Cisbani E, Frullani S. *SNIFFER system: a multipurpose aerial platform for large area radiological surveillance, emergency management and air pollution monitoring.* Roma: Istituto Superiore di Sanità; 2007. (Rapporti ISTISAN 07/33).

Presidente dell'Istituto Superiore di Sanità e Direttore responsabile: *Enrico Garaci*
Registro della Stampa - Tribunale di Roma n. 131/88 del 1° marzo 1988

Redazione: *Paola De Castro, Sara Modigliani* e *Sandra Salinetti*
La responsabilità dei dati scientifici e tecnici è dei singoli autori.

TABLE OF CONTENTS

INTRODUCTION

The uncontrolled re-entry in the atmosphere of nuclear powered satellites from the end of 70s to the beginning of 80s pointed out the need of monitoring systems able to scan, in a relatively short time, large extensions of potentially contaminated territories.

In Italy, the Istituto Superiore di Sanità (National Institute of Health) in a framework of collaborative research programme between its Laboratory of Physics and the Atomic Defence Laboratory of Corpo Nazionale dei Vigili del Fuoco (Italian Fire and Technical Rescue Brigade) developed a system mounted in an antivibrating frame under the fuselage of an Agusta-Bell 412 helicopter.

The accident of April the 26th 1986 at the Chernobyl nuclear power plant made evident on one side the need of an aerial platform for large scale and rapid radiological monitoring, and on the other side the limits of the helicopter and its on-board equipment.

Based on the Chernobyl emergency lesson, the Italian Institute of Health in collaboration with the Ministero dell'Ambiente (Ministry of Environment) considered the development and implementation of a multipurpose air sampling system based on a fixed wing aircraft.

After several years of research and development, such a system, called SNIFFER, has recently passed its first tests, has been authorized by the Italian Airworthiness Authority (ENAC, Ente Nazionale per l'Aviazione Civile) and is now ready for commissioning. Hosted on a fixed wing, small aircraft, it is based on an air sampling system, working in the isokinetic condition and integrating two small in-line beta and gamma radiation detectors and on off-line high resolution gamma detector, that permit a quantitative estimation and identification of the sampled air radioactivity. A large scintillator crystal, separated from the sampling line is capable of air and on-ground radioactivity detection. The combination of the data from the different detectors allows a quantitative estimation of the air and ground contaminations.

In addition to the radiological surveillance, the same aerial platform is efficiently exploited for the study and monitoring of urban pollution. The SNIFFER is equipped with two samplers that permit an off-line evaluation of aerosol and some chemical polluting sources concentration on the sampled air.

The present report is devoted to the description of the SNIFFER.

In the first chapter, the motivations behind the SNIFFER origin are discussed, focusing mainly on the Chernobyl accident and its characteristic large scale emergency.

The second chapter presents the requirements that a system devoted to radiological surveillance (and air pollution monitoring) on medium/large scale and responding to emergency like Chernobyl should have. Moreover, the main aspects of the design (such as the aerial platform, the isokinetic condition and the analytical derivation of the pollutant concentrations) are discussed.

In the third chapter the SNIFFER implementation, components and software, are described in details.

Eventually, in the last chapter, the next project steps and improvements are shortly discussed.

FROM CHERNOBYL ACCIDENT TO NEW SOLUTIONS FOR RADIOLOGICAL EMERGENCY AND AIR POLLUTION MONITORING

The accident of April the 26th 1986 at the Chernobyl nuclear power plant, was the most severe event occurred in the nuclear industry. The accident caused the deaths within few days or weeks of 30 power plant employees and firemen and at least 19 more in the following years. About 240,000 workers (the so-called "liquidators") were called upon in 1986 and 1987 to take part in major mitigation activities at the reactor and the 30-km zone surrounding the reactor; residual mitigation activities continued until 1990. All together, about 600,000 persons received the special status of "liquidator". Due to the huge area affected by the accident, about 116,000 people have been evacuated (1). The released radioactive material (consisting of gases and dusts) was transported over a large part of the European continent, being potential risk to hundreds millions of people.

Although precise quantitative estimation of the effects on humans are still debated, several years after the Three Mile Island accident in the United States, the Chernobyl accident in 1986 completely changed the public perception of nuclear risk. While the first accident provided the impetus to develop new research programs on nuclear safety, the second, with its human deaths and the dispersion of a large part of the reactor core into vast regions, raised a large number of "management" problems, not only for the treatment of severely exposed persons, but also for the decisions that had to be taken in respect of the population (2) during the emergency.

To face these issues, the Italian Institute of Health and the Italian Ministry of Environment sponsored the development of an air sampling system (named SNIFFER) for time-effective, large areas radiological surveillance and monitoring.

Soon, the SNIFFER monitoring capabilities have been extended to the sampling of air pollutants, another relevant risk factor for human health.

The present chapter is an overview of the relevant aspects tacked by the SNIFFER system: the Chernobyl accident is reviewed in term of the geographical and temporal development of its released material; then the effects of the atmospheric pollutants on human health is shortly introduced.

Geographic diffusion of the contaminants after the accident

The Chernobyl nuclear power station is located in the Ukrainian Soviet Socialist Republic in the western USSR, near the boundary with the Byelorussian Soviet Socialist Republic, about 100 km northwest of Kiev and 310 km south-east of Minsk, on the River Pripyat. Neighbouring countries Poland and Romania are 450 km far away (3).

The nuclear accident occurred during a low-power engineering test of the Unit 4 reactor. Safety systems had been switched off, and improper, unstable operation of the reactor caused an incontrollable power surge. The sudden increase in heat production ruptured part of the fuel and small hot fuel particles, reacting with water, caused steam explosion, which destroyed the reactor core. A second destructive explosion occurred two to three seconds later.

The two explosions threw fuel, core components and structural items and graphite into the air producing a shower of high radioactive debris and exposing the destroyed core to the atmosphere. The plume rose up to about 1 km into the air. The heavier debris in the plume was deposited close to the site, but lighter components, including fission products and virtually all the noble gas inventory were blown by the prevailing wind to the North-West of the plant.

In spite of the studies and the efforts spent there are still perplexity and uncertainties on the real dynamic of the facts and the circumstances that led to the accident and on mechanisms that drove its evolution.

Measurements performed on ground after the accident identified the three main high contaminated areas (spots) in the surrounding of the plant, described in Table 1 (2).

Table 1. The three spots identified near the reactor plant

Spot	Areas	^{137}Cs surface contamination (kBq/km^2)	When contamination occurred
Central	30 km around the reactor Large areas of the Northern part of Ukraine and of the Southern part of the Belarus	1,500 40	Initial, active stage of the release
Briansk-Belarus	Interface of the Briansk region of Russia and the Gomel and Mogilevregions of Belarus	Reaches 5000 in some villages	April 28th-29th as a result of rainfall
Kaluga-Tula-Orel	Approximately 500 km north-east of the reactor	Less than 600	April 28th-29th as a result of rainfall

After the accident and the diffusion of radioactive substances outside the three main spots in the greater part of the European territory of the Soviet Union, there were many areas of radioactive contamination with ^{137}Cs levels in the range 40 to 200 kBq/m^2. Overall, the territory of the former Soviet Union initially contained approximately 3,100 km^2 contaminated by ^{137}Cs with deposition levels exceeding 1,500 kBq/m^2; 7,200 km^2 with levels of 600 to 1,500 kBq/m^2; and 10,300 km^2 with levels of 40 to 200 kBq/m^2 (2).

Radioactive particles emitted during the accident were transported by stream flow along thousand kilometres. Atmospheric conditions, particles properties and release height influenced transport on a large scale.

At the time of the accident, surface winds at the Chernobyl site were very weak and variable in direction. However, at 1,500 m altitude the winds were 8-10 m/s from south-east. The initial explosions and heat from the fire carried some of the radioactive materials to this height, where they were transported by the stream flow along the western part of the USSR toward Finland and Sweden. The arrival of radioactive materials outside the USSR was first noted in Sweden on 27th April. The transit time of 36 hours over a distance of some 1,200 km indicates transfer at an average wind speed of 10 m/s (3).

According to aircraft measurements within the USSR, the plume height exceeded 1,200 m on April the 27th, with the maximum radiation occurring at 600 m but on subsequent days, the plume height did not exceed 200-400 m. The volatile elements iodine and caesium, were detectable at greater altitudes (6-9 km) with traces also in the lower stratosphere. Other elements such as cerium, zirconium, neptunium and strontium were for most part of significance only in local deposition within the USSR.

Changing meteorological conditions, with winds of different directions at various altitudes, and continuing releases over a 10-days period resulted in very complex dispersion patterns.

The initial plume arrived on April the 27th in Sweden and Finland (Table 2).

Table 2. Development of the radioactive plume during the first days after the Chernobyl accident

Date	Areas interested by the plume arrival
April 26th	Immediately surronding the core (plume A in Figure 1)
April 27th	First plume observaton in Sweden and immediately after in Finland. A portion of this plume was observed in Poland and in the German democratic Republic
April 29th and 30th	All the eastern and central countries became affected by the plume (plume B in Figure 1)
April 30th	First evidence of the plume arrival in north-east Italy and Switzerland
May 1th	Dectatable activity in France, Belgium and Netherlands
May 2th	Plume arrival in the United Kingdom and in the north of the Greece Detectable activity in the south of the Greece
Early May	Airborne activity reperted in Israel, Kuwait and Turkey

A portion of this plume at lower altitude was directed southward to Poland and the German Democratic Republic. Other eastern and central European countries became affected on April the 29th and 30th. During these days plumes entered Italy and other countries of Central and East Europe. On May the 1st plumes entered Belgium, France and Netherlands; on May the 2nd contamination was revealed in Japan, on May the 4th in China, on May the 5th in India, Canada and United States. No airborne activity from Chernobyl was reported in the southern hemisphere.

The plumes of contaminated air that spread over Europe are described in a highly simplified manner in Figure 1 (3), along with the reported initial arrival times of radioactive material. Figure 2 (2) shows plumes patterns until May the 6th on the basis of ARAC (U.S. Atmospheric Release Advisory Capability) models.

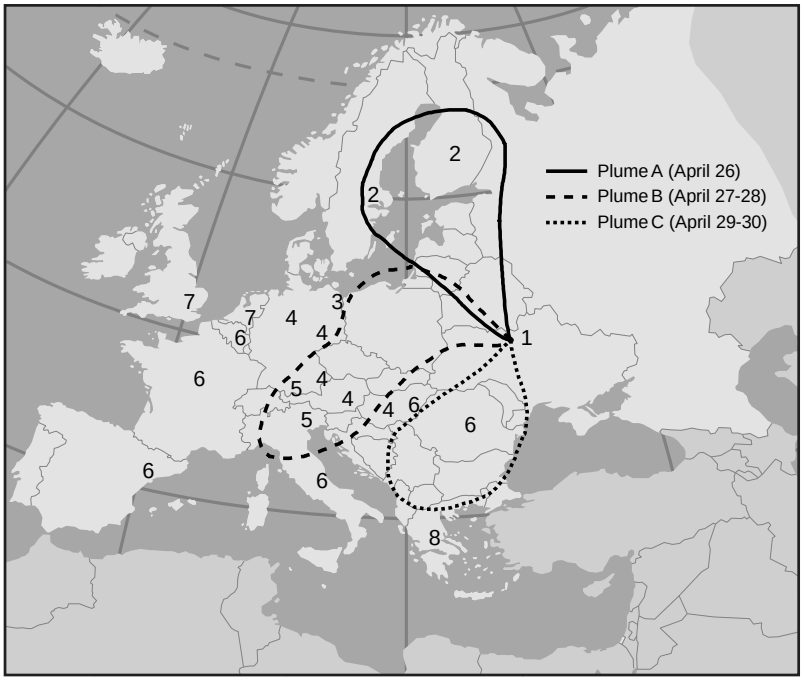

Figure 1. Descriptive plume behaviour; the numbers respresent the first day of excess air activity in each area (1 is April the 26th, 8 is May the 3rd)

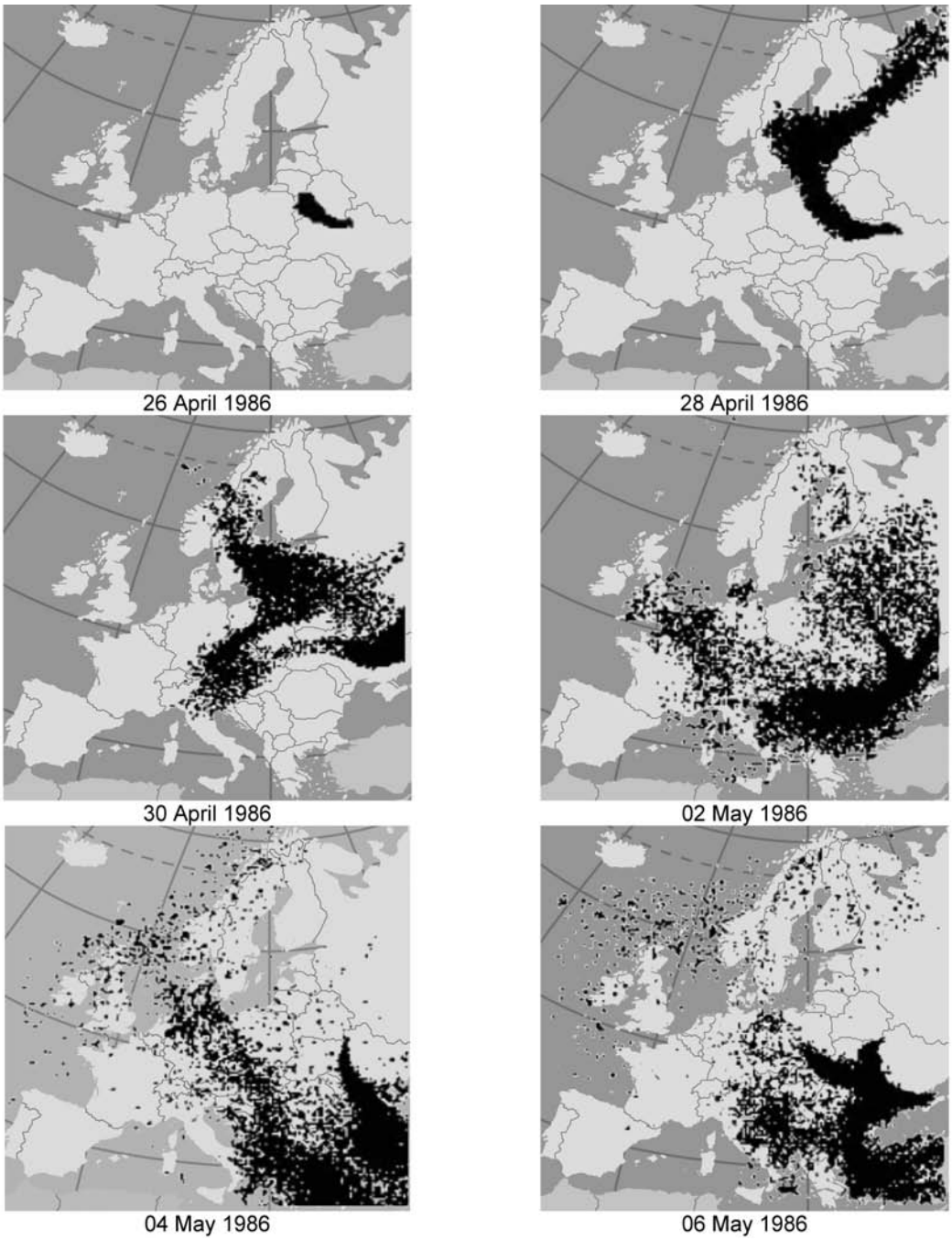

Figure 2. Areas reached by the main body of the plume during the days following the accident (April 26th-May 6th)

Eventually the entire boreal hemisphere was contaminated by material released during the Chernobyl accident. The order of magnitude of the contamination has been deduced from the measurement of the ^{137}Cs isotope due to its long lifetime that permits an easy quantification of its activity. Indeed it is the element that mainly contributes to the dose received by population

when the short lived isotope ^{131}I had decayed. In fact, during the first weeks after the accident the activity deposited on ground was mostly due to short-lived radioisotopes such as ^{131}I.

The ^{137}Cs ground contamination in Europe was characterized by irregularities in the on ground deposition. Relatively high contamination levels were found even very far from the scene of the accident. Such characteristics give a clear idea of the complexity of the contaminants diffusion processes. In a very strong manner they depend on the atmospheric conditions and the orography of the territory interested by the plume (4).

It is evident from the previous short review that such dramatic emergency requires radiation monitoring systems (for atmospheric and on ground contamination determination) able to span large areas in short time.

Radionuclide release and temporal evolution after the accident

In the initial assessment of releases made by the Soviet scientists and presented at the IAEA Post-Accident Assessment Meeting in Vienna (IA86), it was estimated that 100% of the core inventory of the noble gases (Xenon and Krypton) was released, and between 10% and 20% of the more volatile elements of iodine, tellurium and caesium. The early estimation for fuel material released to the environment was (3.0 ± 1.5)% (IA86). This estimation was later revised to (3.5 ± 0.5)% and corresponds to the emission of 6 tons of fragmented fuel.

More data were available when, in their 1988 report (UN88), the United Nations scientific Committee on the effects of Atomic Radiation (UNSCEAR) provided release figures based on worldwide deposition.

Structural damages of the building and core reactor caused the diffusion of an enormous amount of radioactive material. The release, however, did not happen only just after the event, but followed a very singular temporal sequence.

In fact, only 25% of the diffused material was released during the first day of the accident, the rest in a period of nine days. Soviet experts succeeded to reconstruct the entire relative sequence of the release process, as shown in Figure 3 (2), which was characterized by different phases:

1. During the first day after the accident the diffusion of the radioactive material was the result of the explosions in the reactor and of the fire in the Unit 4;
2. Second phase covers a period of 5 days from the accident during which the release rate is approximately 6 times smaller than the first phase;
3. From the sixth to the tenth days the release rate increase again to about 70% of the initial release rate; an emission of volatile elements was observed. These phenomena were attributed to heating of the fuel in the core to above 2000°C, owing to residual heat release;
4. A sudden drop in the release rate nine days after the accident to less than 1% of the initial rate. This final stage was characterized by a rapid decrease in the emission of fission products and a gradual termination of discharges. These phenomena were the consequences of the special measures adopted, which caused the fission products to be included in compounds that were chemically more stable.

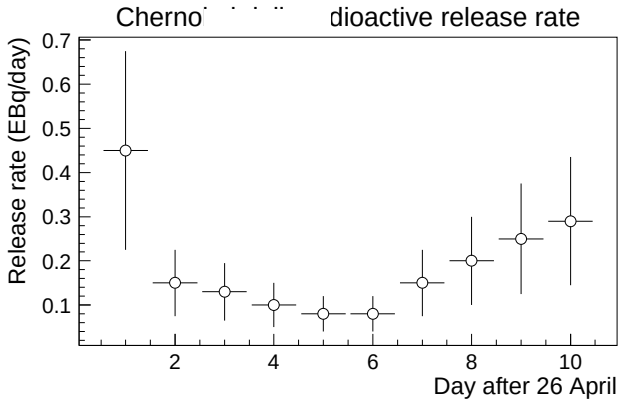

Figure 3. Daily release rate to the atmosphere of radioactive materials, excluding noble gases, during the Chernobyl accident. (values are decay-corrected to 6 May 1986 with uncertainty of ± 50%)

Contamination in Italy and the activity of the Istituto Superiore di Sanità

Aerial Radiological Measuring Systems (ARMS) developed in the late 1950s for uranium ore prospecting provided an invaluable tool in environmental surveillance of nuclear power plants and nuclear processing facilities as well as in emergency response for large-scale radiological accidents. Historically the international concern of the potentialities of such systems was triggered in 1978 by the search and partial recovery of radioactive debris scattered over an estimated area of about 100,000 km^2 as a consequence of the impact in the northwest territories of Canada of the nuclear powered Soviet "COSMOS-954" satellite. In 1983 another nuclear powered satellite "COSMOS-1402" spread large quantity of radioactive material. From these events it was evident that Italy and many other countries with the exception of United States, Canada and Sweden was not able to face emergencies connected with uncontrolled re-entry in the atmosphere of nuclear powered satellite or with orphan/lost sources when debris are scattered over very large areas (5) or with recovery of a orphan/lost source whose search can span over many square kilometres.

At the beginning of the 80s the Laboratory of Physics of the Istituto Superiore di Sanità, in collaboration with the Atomic Defence Laboratory of the Corpo Nazionale dei Vigili del Fuoco (5, 6), studied the feasibility of a radiological monitoring system to be mounted on aircrafts to face emergencies with contamination of very large areas that cannot be surveyed in the short timescale (required by the emergency) by ground based search systems due to extension and sometime accessibility. It considered three main tasks:

1. search of localized but spread over large areas source;
2. search of orphan or lost sources;
3. measurements of ground contamination derived from pacific or non-pacific use of nuclear energy.

Within the budget of the research programme the developed system consisted of a large (16"×4"× 4") NaI(Tl) detector module mounted in an antivibrating frame under the fuselage of

an Agusta-Bell helicopter (Figure 4) (6). Its control and acquisition system was also installed on board in the space left by the removal of a row seats.

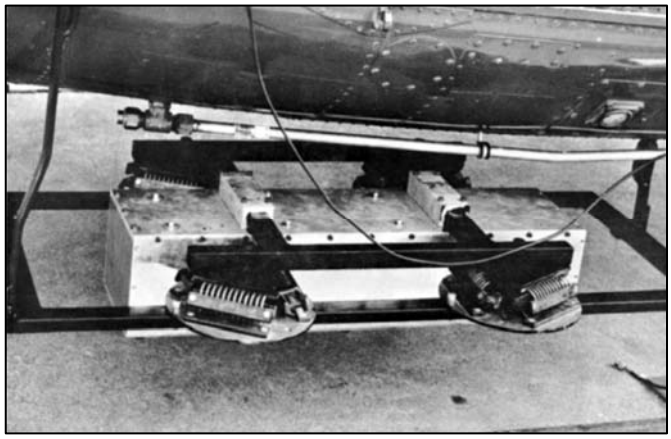

Figure 4. Anti-vibrating frame where was hosted NaI scintillator

The sizeable on-board electronic control system (Figure 5) (6) was made of a Tennelec TC948 power pack, an Ortec 572 Amplifier and an analog to digital converter LeCroy 3511; the data acquisition was managed by a LeCroy Minicomputer allowing data storage on floppy disks.

Figure 5. The bulky control system hosted on Agusta-Bell 412 helicopter

Such aerial monitoring system permitted a series of missions during the Chernobyl emergency, between the beginning of May and mid June of 1986, covering most of the Centre-south of Italy. While the presence of contamination was clearly seen since the first mission and the identification of the main radioisotope groups as well as the change in their composition with time was possible, a quantitative assessment on the contamination parameters had not been possible until the mission the 21st of May.

In Figure 6 the integral counts under the last two peaks of the spectra are reported as measured during the missions between the 3rd and the 21st of May in the different areas flown in the time sequence (6). There is a clear evidence of a systematic increase with time of the detected radioactivity in the first two missions due to the accumulation of contamination of the helicopter fuselage while flying in the plume. Also in the mission on the 9th of May, some radioactivity was still present in air because measurements done at different height did not scale according to the function expected when the source of contamination was dispersed at ground level.

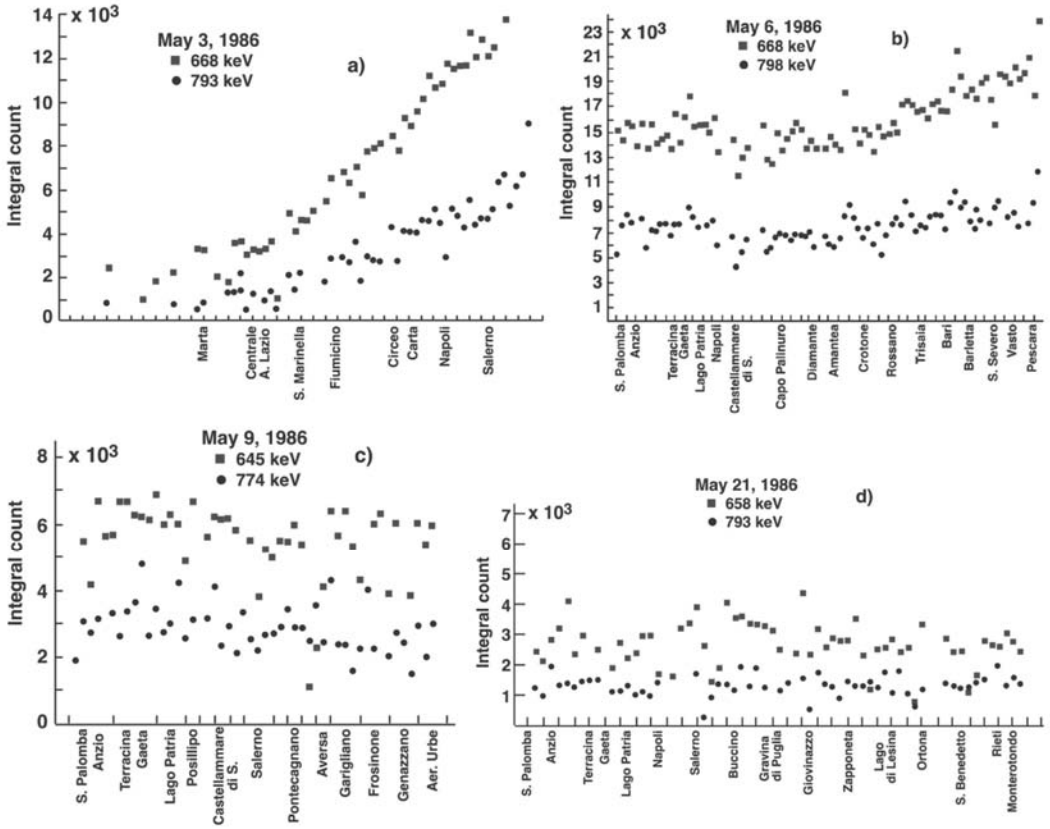

Figure 6. Integral counts under the two higher energy peaks during the flight missions in the date indicated

On the 21st of May, for the first time, the measurements taken at different heights successfully passed all the tests of consistency, and the quantitative determination of the level of ground contamination was possible (Figure 7) (6).

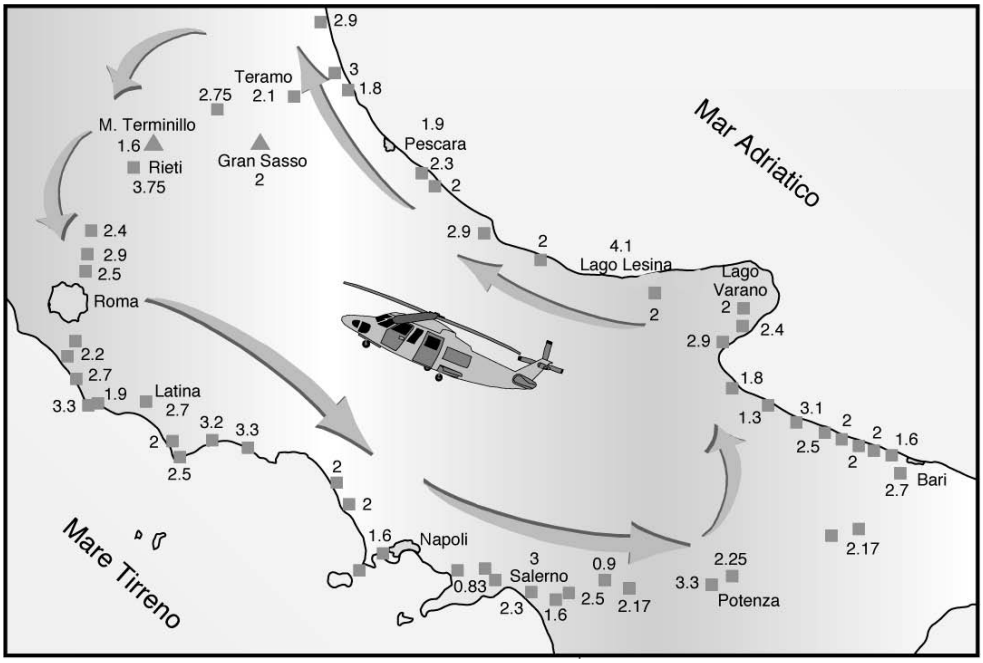

Figure 7. ^{134}Cs (kBq/m^2) ground contamination derived from measurements of May the 21st mission

This experience demonstrated the severe limits during the early phase of a nuclear emergency of an aerial platform equipped with radiation detectors developed for ground contamination measurements: the first quantitative measurement of contamination parameter was only possible after many days from the beginning of the accident.

These systems allow the quantification of the source activity, or the ground contamination, through the analysis of the gamma ray spectra measured, only under the assumption of very limited and specific source patterns (point-like for a single source, diffused over a surface for ground surface contamination). In case of a more complex (and realistic) situation, there is not a suitable knowledge to model the radiation source; therefore, the measurements can only supply qualitative information. This is the case, both in near and far field, when the radioactive plume released by an accident is passing over a Country. The lack of quantitative measurements and the derived uncertainty in forecasting the propagation of the radioactive contamination do not help the emergency management in the most critical phase, i.e. when countermeasures have to be decided in a preventive way and some risk of negative effects is inevitably linked to their enforcement.

A more powerful (and predictive) tool for the emergency management is provided by an aerial platform instrumented for in-plume measurements, aiming to characterize the extension, composition and concentration of the radioactive mixture in the plume, as well as to measure *in situ* meteorological parameters that can be of invaluable help in emergency early phase.

Atmospheric organic pollutants and their effects on human health

In developed Countries, in the last twenty years, greater attention has been turned to problems related to air pollution and wide interest has grown relatively to the air quality control.

A series of European Community directives and corresponding Italian decrees (7-9) contributed to the reduction of pollutant concentrations in all the States. These laws impose severe limits on the emissions of the principal polluting sources (vehicular traffic and industry). Such emissions mainly consist of VOCs (Volatile Organic Compounds) and PAHs (Polycyclic Aromatic Hydrocarbons).[1]

Among atmospheric pollutants, the anthropogenic organic species have great importance with enormous impact on

– *Atmosphere*
  - In high populated areas, anthropogenic VOCs are often more abundant than natural ones.
  - Chemical composition of the anthropogenic emissions is very different from the composition of the natural atmosphere, whether in concentration or composition terms.

– *Human health*
  - Organic species present in aerosols, many of which have carcinogenic or mutagenic effects (chlorine, nitrogen and sulphur compounds, benzo[a]pirene and polycyclic aromatic hydrocarbons), are contained almost totally in the inhalable fraction of powders.

It is commonly known that air pollution constitutes one of the main risk factors for human health and has negative influence on many diseases. In the meantime air pollution speed up the deterioration of exposed materials and buildings, compromise cultivation and vegetation and produce climate alterations (10).

The effects that air pollutants have on human health are charged to various organs and apparatuses and can vary according to pollutant considered and according to its mechanism of action. Warnings of an excess of tumours are of particular interest, principally, charged on respiratory apparatus in the high populated areas.

Both radiological surveillance and atmospheric pollution monitoring share the same basic need: survey extended geographical areas in a time-effective way. This fact has been considered during the design of the SNIFFER, ending up with a multi-purpose system based on a fixed wing aircraft platform as detailed in the next two chapters.

1 PAHs are chemical compounds that consist of fused benzene rings. They are the most widespread organic pollutants. Some of them are known or suspected to be carcinogens, and are linked to other health problems. They are primarily formed by incomplete combustion of carbon-containing fuels such as wood, coal, diesel, fat or tobacco. VOCs are organic chemical compounds that have high enough vapour pressure under normal conditions to significantly vaporize. A wide range of carbon-based molecules, such as aldehydes, ketones and hydrocarbons can be considered VOC. Some of them are suspected carcinogens and may lead to leukaemia through prolonged exposure. Some VOCs react with nitrogen oxides in the air in the presence of sunlight to form ozone. Vapours of VOCs escaping into the air contribute to air pollution.

SNIFFER SYSTEM: GENERAL ARCHITECTURE, REQUIREMENTS, AND GUIDELINES

The Chernobyl emergency clearly showed that the quantitative evaluation of the release during a radiological accident and the forecasting of the plume development, require large scale aerial measurements during the early phases of the emergencies, integrated with ground based data.

In response to this need, Istituto Superiore di Sanità (ISS) has been developing since then a sampling and measuring system, called SNIFFER hosted on an aerial platform.

The SNIFFER performs isokinetic sampling with the suction of air samples and their collection on in-line filters, where their activity are measured and gamma radioactive sources identified.

A GPS (Global Positioning System) module, mounted on board, allows the geolocation of the acquired data in a space-temporal reference.

To efficiently exploit the aerial platform, the SNIFFER is also equipped with particulate and injurious gases sampling devices, that are of great relevance in air quality control; their routinely monitoring (on large regions) basically requires the same platform of the radiological surveillance.

The SNIFFER system has originated from the above needs; therefore its main purpose is the large area – short time scale – radioactive contamination surveillance and pollution monitoring for emergency management and routine operations.

The general architecture of the SNIFFER has identified in the following three main functional blocks:

- The aerial platform that hosts the detection equipment and must allows: a large area of surveillance in short time and the isokinetic sampling of the aerosol (relevant for quantitative estimation as discussed later).
- The radioactivity contamination measurement (aerial and on-ground) that includes the identification of the radioactive gamma sources and the quantitative estimation of the related activities.
- The particulate and injurious gases monitoring, that provides PAH and VOC sampling and particulate characterization.

It is worth mentioning that these blocks are inter-dependant:

- The quantitative estimation of the radioactivity and aerosol components demand for an isokinetic sampling.
- The isokinetic sampling is obtained using the proper aerial platform (fixed wing), a properly designed suction line and dynamically controlling the air flow through it.
- The aerosol sampled filter is analyzed in term of radiation (for radioactive contamination) and particle composition (for particulate characterization).

In this chapter the relevant design aspects of each block is shortly presented: relevant requirements, adopted guidelines and solutions are discussed.

The aerial platform

The sampling platform must comply with some constraints demanded by sampling methodology and operative conditions. The sampling probe has to be located in a place where aerodynamic perturbation induced by the movement of the platform is negligible. This requirement calls for a fixed wing aircraft to avoid effects of rotor blades on the surrounding air velocity field and for a plane which offers the possibility to install the SNIFFER in its front part with the probe located ahead of the aircraft.

The profile of the front cap of the airplane must be modified to allocate the sampling unit. Safety conditions for the flights must be satisfied at an altitude range from some tens of meters to a few kilometers while take off and landing operations should be possible in a grass type airstrip of a few hundreds meters (Short Take Off and Landing – STOL type aircraft).

These requirements are fulfilled by the Sky Arrow 650 – manufactured by Iniziative Industriali Italiane SpA (Rome, Italy) in its RAWAS (Remotely Assisted Working Aerial System) and ERA (Environmental Research Aircraft) versions – which is certified by National Airworthiness Authorities for territory and environmental research/monitoring and “Electronic News Gathering”.

Entirely made of advanced composite material, the structure is corrosion free, strong yet light weight. The non-structural part of the fuselage can be remodelled to a certain degree to locate the instrumentation. It is designed for operating in open space networking and can be integrated into the most updated communications technologies available.

Figure 8 shows a Sky Arrow I-TREO airplane equipped with the SNIFFER system: visible are the front probe and, on the side of the fuselage, the cooling dewar of the HPGe detector.

Eventually, the equipment hosted in the aircraft is constrained by space, weight and power consumption.

Figure 8. Sky Arrow 650 I-TREO in flight during the test session needed to obtain ENAC certification

Isokinetic sampling

The in-plume direct sampling of the probe (installed on fixed wing aircraft) must be operated according to precise criteria that guarantee the representative and significance of the gathered data. In this respect, the sampling has to ensure isokinetic conditions, i.e. the inlet walls of the sampler shall be parallel to the gas streamlines and the gas velocity entering the probe (v) shall be identical to the free stream velocity entering the inlet (v_0). This is equivalent to the absence of deformation of the stream lines in the neighbourhood of the inlet. A failure in the isokinetic sampling may result in a distortion of the size distribution and a misrepresentation of the concentration.

In Figure 9 air stream behaviour at probe entrance, when the isokinetic condition ($v_0 = v$) is met and when is not satisfied ($v_0 < v$ or $v_0 > v$), is shown (11).

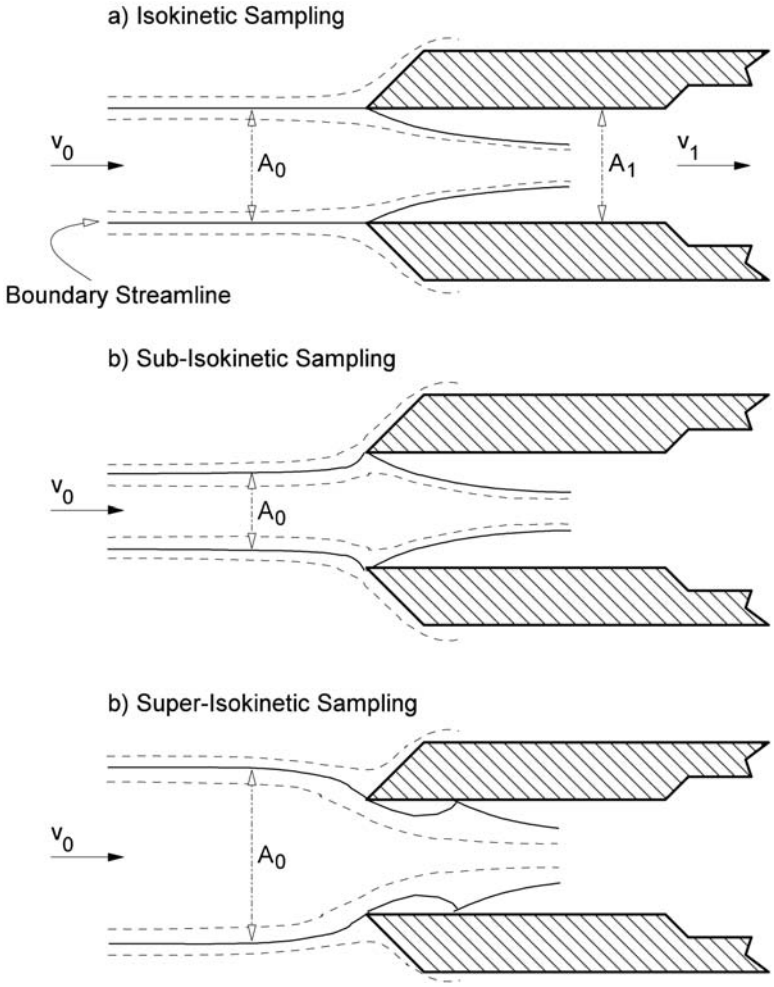

Figure 9. Air sampling through probe. Isokinetic condition is ensured when air external velocity respect to the aircraft (v_0) is equal to its velocity when entering the probe (v)

To have an isokinetic sampling, the velocity of the entering stream must be adapted to that of the external air (relative speed of the aircraft respect to the air) through a continuous regulation

of the inlet flow rate according to the operative and environmental conditions (aircraft speed, pressure and temperature).

The SNIFFER system, therefore, must have a sampling line with a flow regulation operated by an automated control unit that, by means of sensors measuring the relevant environmental parameters, can assure isokinetic sampling. The control software shall regulate the suction of the air and compute the needed sampled air volume in the current and nominal (STP, Standard Temperature and Pressure) conditions.

The aircraft speed is measured by a Pitot-Prandtl tube mounted in the front part of the aircraft below the sampling probe. It consists of two, coaxial, cylindrical tubes. The inner tube entrance point along the aircraft direction, and allows the streamlines to enter and to be brought to rest at the pressure sensor. The second outer tube entrance consists of a series of small holes drilled on the tube surface, perpendicular to its axis, and therefore perpendicular to the direct airflow. The outer tube is pressurized by the local random component of the air velocity, that is the static pressure. Instead the pressure of the streamlines along the inner tube, called stagnation or total pressure, is the sum of the static pressure and the component of dynamic pressure due to the stream (relative to the aircraft) velocity.

The maximum aircraft speed is well below 0.3 Mach (30% of the sound velocity in air) that is the value usually assumed for transition between incompressible and compressible airflow. Daniel Bernoulli equation can be applied:

$$p_{stagnation} = p_{static} + \frac{1}{2}\rho v^2$$

being ρ and v the air density and aircraft/wind speed, respectively. The inner and external parts of the Pitot-Prandtl are connected to a differential pressure gauge whose measurement Δp gives directly the aircraft/wind speed:

$$v = \sqrt{\frac{2(p_{stagnation} - p_{static})}{\rho}} = \sqrt{\frac{2\Delta p}{\rho}}$$

Expressing ρ in kg/m^3 and Δp in Pascal, v is expressed in m/s.

The air density is determined through the temperature T and pressure p measurements of the sampled air and assuming the validity of the equation of state for a perfect gas:

$$p = \rho RT$$

being R the universal constant for a perfect gas (=8.314 J/K).

Then from the relation:

$$\frac{\rho}{\rho^*} = \frac{pT^*}{p^*T}$$

the aircraft/wind speed is derived:

$$v = \sqrt{\frac{2\Delta p}{\rho}} = \sqrt{\frac{2\Delta p p^* T}{\rho^* pT^*}}$$

where p* and T* are values of pressure and temperature at which the air density ρ* is known from well established measurements [ρ*= 1.292 at STP (0 °C and 101.325 kPa); ρ*= 1.168 at 25 °C and 100 kPa].

Along the SNIFFER line a Venturi tube (Venturi meter) measures the actual volumetric flow rate by measuring the differential pressure across a calibrated resistance (a streamlined constriction in the duct to minimize losses) in the flow stream.

The Venturi meter also provides pressure and temperature in order to obtain the volumetric flow at STP.

The continuity equation equates the mass flows at entrance (ϕ_M) and at the Venturi ($\phi_{M,Venturi}$):

$$\phi_M = \phi_{M,Venturi}$$

On the other hand, the mass flow is proportional to the volumetric flow (ϕ_V) via the density:

$$\phi_M = \rho \cdot \phi_V$$

and the volumetric flow is proportional to the flow speed (v) via the cross section (A) of the tube:

$$\phi_V = v \cdot A.$$

Combining the above three simple relations, the sampling is isokinetic when the following condition is maintained (through the control of the needle valve that increase or decrease the impedence of the line):

$$\phi_{V,Venturi} = \frac{\rho}{\rho_{Venturi}} \cdot v \cdot A$$

or introducing the temperature and pressure:

$$\phi_{V,Venturi} = \frac{p \cdot T_{Venturi}}{T \cdot p_{Venturi}} \cdot v \cdot A$$

where, the parameters with the Venturi subscript are measured at by the Venturi Meter, while the other are measured at the suction line entrance.

The whole sampling line is schematically shown in Figure 10, where the environmental parameters (of the previous equation) used to control the isokinetic sampling are also indicated: sensors measure the external temperature (T), the total (p) and static pressures in the Pitot-Prandtl canalisations (and derived speed v), the volumetric flow ($\phi_{V,Venturi}$) together with the corresponding temperature ($T_{Venturi}$) and pressure ($p_{Venturi}$). The ejector at the end of the sampling line is used to overcome the impedance due to the filter and other fluidodynamic resistances along the line.

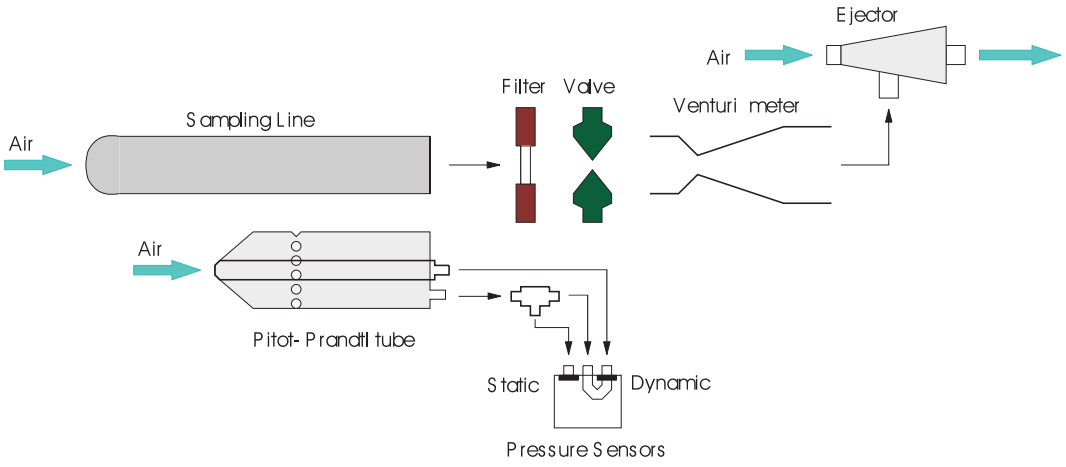

Figure 10. Schematic view of the isokinetic sampling line of the SNIFFER

Radioactive contamination: radionuclide identification

An effective radioactive measuring system that uses a probe for air sampling must be able to provide real-time quantitative evaluation of the collected radioactive pollutants.

The main radioactive elements to be taken into account are those characteristic of a nuclear accident with an atmospheric release of fission products or radioactive elements in general. They are shown in Table 3 with energies of emitted gamma and beta rays, expressed in MeV.

Table 3. Most relevant radioactive elements that can be released after a nuclear accident and related energies of the emitted gamma and beta rays

Element	Emitted energy (MeV)	
	Beta rays	**Gamma rays**
Cobalt^{60}	*0.31 max(99%)*	1.17 e 1.33 (100%)
Kripton^{85}	*0.69 max*	0.51 (0.4%)
Iodium^{131}	*0.61 max (89%)*	0.36 (81%)
Caesium^{137}	*0.51 max(95%)*	0.66 (85%)
Strontium^{90}+Yttrium^{90}	*0.55 max e 2.3 max*	-
Cerium^{14}+Praseodymium^{144}	*0.31 max (76%) e 3.0 max (98%)*	-

Other radioactive elements released during an accident have a smaller importance because of their short mean life (^{133}Xe, ^{135}Xe and ^{41}Ar); however it is possible to forecast their sampling (because they are gases) using adsorption systems on active carbon filters.

While beta and gamma ionizing radiation is quite common (the elements in Table 3 are beta and gamma emitters) and conveniently detectable, the alpha and neutron radiation are hard to be detected by on-aircraft instrumentation.

The identification of gamma emitting radionuclides demands high resolution systems and therefore relatively large volume of detection. Such systems, therefore, cannot be positioned along the sampling line since they would cause a clogging of the line itself.

The solution adopted to avoid such type of problems consists in the use of two detectors: the position along the suction line of small detectors with course resolution that is used to trigger in real time the occurrence of a certain anomaly (presence of contaminants) respect to background. The high resolution detector is located out of the sampling line (see next chapter) and provides slightly delayed information on the composition of the contaminants.

In addition to the air activity excess and radionuclide identification the aerial platform must be able to estimate the on-ground contamination. In order to do that, the platform shall host a large (efficient) volume detector[2] whose acquisition shall be synchronized with the other detectors. The next section presents the relevant theoretical aspects of the aerial based ground contamination measurement.

[2] Typically for such a type of spectral analysis the commercial and relatively inexpensive NaI(Tl) scintillator crystal is preferred.

Radioactive contamination: measurements from aircraft of ground radioactivity

The analytical evaluation of the on-ground contamination by a properly equipped aircraft requires some hypotheses on concentration of the contamination and on flight geometry.

We assume a cuboid scintillation crystal detector mounted on the aircraft and suppose that the detector is able to reveal all the gamma rays contained within a spherical volume of radius *R*. The detector is positioned in the centre of such spherical volume (Figure 11):

- if *R* is smaller than the aircraft altitude, the detector will measure exclusively radiological contamination from sources in air and assuming a model of uniform air contamination could provide quantitative information on the radiological situation;
- if *R* is greater than the aircraft altitude, the detector will measure contributions coming from both air and ground contaminations and quantitative assessment becomes impossible.

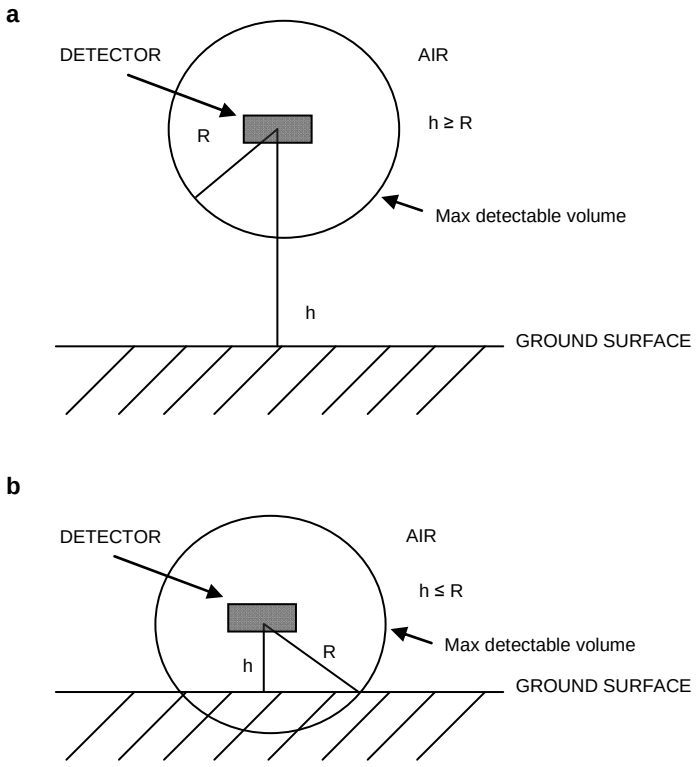

Figure 11. Definition of geometric parameters of the SNIFFER system: R<h (a); R>h (b)

In the following, different situations, with increasing degree of complexity, are taken into account. Analytical evaluation will start from a simple gamma emitter point-like source; then a surface of uniform activity (with thin and thick detector block) will be considered. Finally the situation when both air and ground contaminations are present is discussed. The presented analytical expressions are intended to provide a first order evaluation of the real condition, whose accurate estimation requires numerical modeling.

Point-like contamination

In general terms, in case of flying over a source of known activity s in conditions of "hovering", the background subtracted count rate relatively to a gamma peak of defined energy, is given by:

$$N_0 = \frac{\eta s A_{inf}}{4\pi d^2} e^{-\mu d} \quad [1]$$

where: η = detector efficiency;
s = source strength (photons/s);
A_{inf} = effective detector area (cm^2);
d = distance between the point source and the detector (cm);
μ = photon coefficient of attenuation in air (cm^{-1}).

The measurements carried out in these conditions allow the determination of the detector efficiency, for different energies using suitable sources.

Uniformly distributed surface contamination

In the case of a planar radioactive source, uniformly distributed over a circle of radius r with concentration C_s, all the characteristic parameters of the detection geometry are those defined in Figure 12.

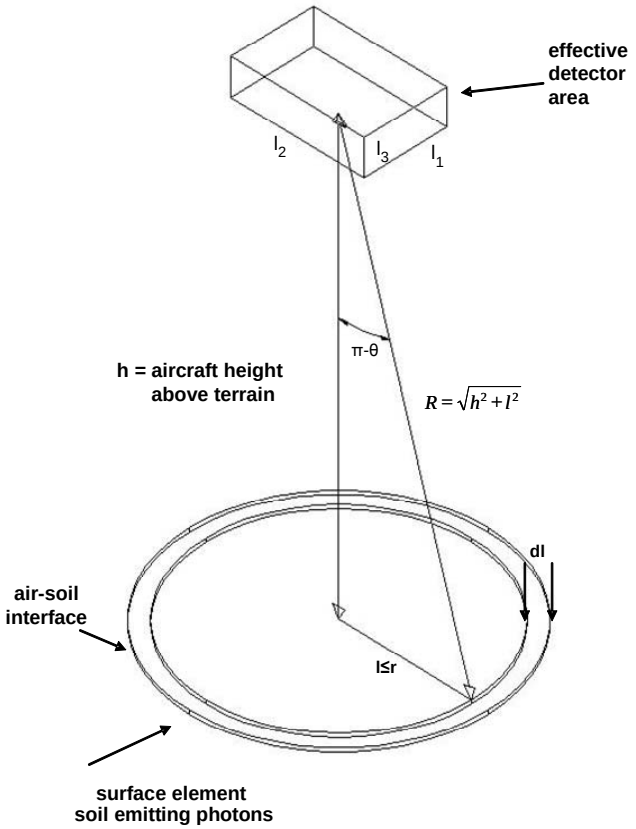

Figure 12. Definition of the characteristic parameters in the aerial detection geometry

Thin detector

Assuming a detector with $l_3 \cong 0$ (vertical size) and l_1 x $l_1 \cong A_{inf}$ (a thin horizontal detector), the relation between counts measured by the detector and ground concentration will be given by:

$$dN_S = \frac{\eta C_S A_{\inf} e^{-\mu\sqrt{h^2+l^2}}}{4\pi(h^2+l^2)} 2\pi l dl \qquad [2]$$

where the new parameters are:

C_s = number of photons emitted by the source for square centimetre of contaminated area (photons/s·cm^2);
h = aircraft altitude;
l = radius of the differential volume ring.

Integrating over $0 \le l \le l_{max}$ we obtain:

$$N_{Surface}^{thin} = \frac{\eta A_{\inf} C_S}{2} E_1(\mu h) \qquad [3]$$

where the exponential integral:

$$E_1(\mu h) = \int_0^{l_{\max}} dl\ I_0(h,\mu)$$

is defined through:

$$I_0(h,\mu) = \frac{e^{-\mu\sqrt{h^2+l^2}}}{h^2+l^2} l\,.$$

Figures 13 and 14 show the above integral exponential values *vs* l_{max} at different altitudes with realistic values of μ for ^{60}Co and ^{137}Cs respectively. It is clear that the ground contaminated surface that contributes to detector counts is contained in a circle of approximately 300 metres (when the curves are almost saturated).

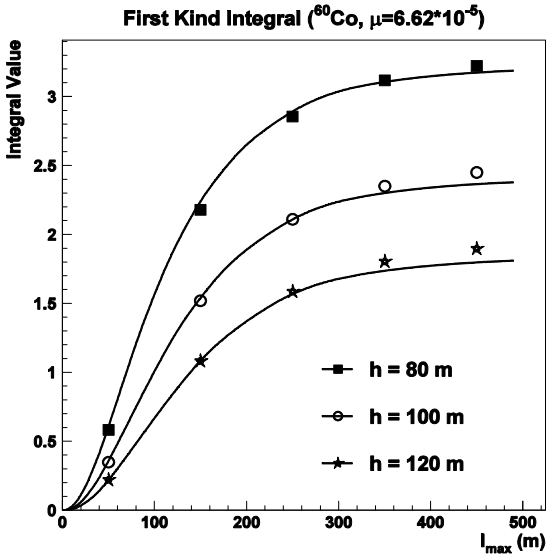

Figure 13. ^{60}Co source: exponential integral values *vs* different height of flight

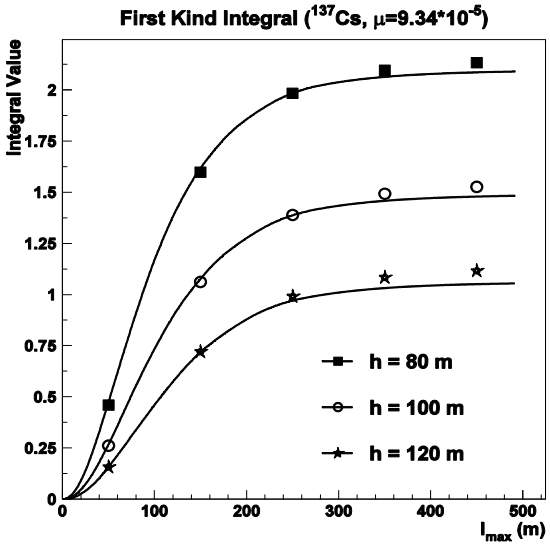

Figure 14. ^{137}Cs source: exponential integral values *vs* different height of flight

From equation [3], the ground contamination of a uniformly distributed source is therefore:

$$C_s = \frac{2N_S}{\eta A_{\text{inf}} E_1(\mu h)} \qquad [4]$$

where all parameters are known, with the efficiency η obtained using a point-like source of well-known activity.

Thick detector

In the more general case of a detector with finite thickness (a parallelepiped of size l_1 x l_2 x l_3 where each size is much smaller than R), the number of photons at a given energy can be estimated exploiting the detector (x, y) symmetries and to distinguish 24 regions (in which the ground area is segmented) (from type 1 to type 6) as shown in Figure 15.

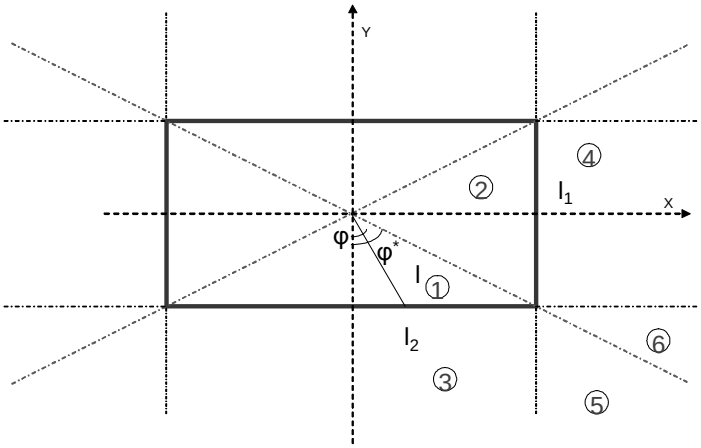

**Figure 15. Top view of the detector ground projection (thick box).
Numbers refer to the different region types where the integration is carried out**

In the following l_x and l_y are the coordinates on the ground projection and:

$$l = \sqrt{l_x^2 + l_y^2} \ .$$

Contribution from type 1 and type 2 regions

There are 4 regions of type 1, defined by:

$$0 \le |l_x| \le \frac{l_2}{2}\,;\ 0 \le |l_y| \le \frac{l_1}{2}\,;\ |l_x/l_y| < l_1/l_2$$

Referring to Figures 15 and 16, it can be deduced that the contribution of these regions comes only from a portion of the bottom side of the detector. In such case, the relation between counts measured by the detector and ground concentration will be given by the integral (dependence on C_s, η, μ, and l_i are implicit):

$$N_1(h) = \frac{\eta\, C_s (l_1 \times l_2)}{4\pi} \int_0^{\varphi^*} d\varphi \int_0^{\frac{l_1}{2\cos\varphi}} dl\ I_0(h,\mu) \sin\left(\theta - \frac{\pi}{2}\right) dl$$

$$= \frac{\eta\, C_s (l_1 \times l_2)}{4\pi} \int_0^{\varphi^*} d\varphi \int_0^{\frac{l_1}{2\cos\varphi}} dl\ I_1(l;h,\mu)$$

where: $\varphi^* = arctg\left(\frac{l_2}{l_1}\right)$, $\theta = \pi - arctg\left(\frac{l}{h}\right)$

and: $I_1(l;h,\mu) = I_0(h,\mu) \sin\left(\frac{\pi}{2} - arctg\left(\frac{l}{h}\right)\right)$

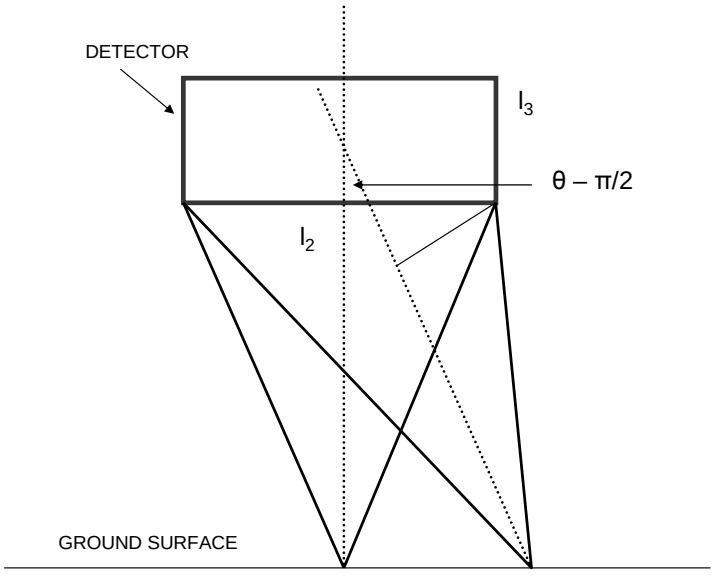

Figure 16. Lateral projection of the detector

For the sake of simplicity, only the dependence on h is expressed in the computed counts.
There are 4 regions of type 2, defined by:

$$0 \le |l_x| \le \frac{l_2}{2};\ 0 \le |l_y| \le \frac{l_1}{2};\ |l_x/l_y| \ge l_1/l_2$$

Still referring to Figures 16 and 17, the counts coming from this region are given by:

$$N_2(h) = \frac{\eta C_s (l_1 \times l_2)}{4\pi} \int_{\frac{\pi}{2}}^{\frac{\pi}{2}+\varphi^*} d\varphi \int_0^{\frac{l_2}{2\cos(\varphi - \pi/2)}} dl\ I_1(l;h;\mu)$$

It is worth noting that the contributions from region type 1 and 2 come only from the bottom face of the detector and are not influenced (first order) by the vertical sides. Then, the total contribution from all regions of type 1 and 2 is:

$$N_A(h) = 4\left(N_1(h) + N_2(h)\right).$$

Contribution from type 3 and type 4 regions

The regions of type 3 are identical under l_1 and l_2 swapping to regions of type 4. All of them are defined by:

$$0 \le |l_x| \le \frac{l_2}{2};\ |l_y| \ge \frac{l_1}{2};\ |l_x| \ge \frac{l_2}{2};\ 0 \le |l_y| \le \frac{l_1}{2};$$

In region of type 3 (see Figure 16) (Figure 17), the relation between counts measured by the detector and ground concentration must account both bottom and l_2 x l_3 side faces:

$$N_3(h) = \frac{\eta C_s}{4\pi}\left\{ \int_0^{\arcsin\left(\frac{l_2}{2r}\right)} d\varphi \int_{\frac{l_1}{2\cos\varphi}}^{r} dl\ \left[(l_1 \times l_2) I_1(l;h,\mu) + (l_2 \times l_3) I_2(\varphi,l;h,\mu)\right] + \right.$$
$$\left. + \int_{\arcsin\left(\frac{l_2}{2r}\right)}^{\arcsin\left(\frac{l_2}{\sqrt{l_1^2+l_2^2}}\right)} d\varphi \int_{\frac{l_1}{2\cos\varphi}}^{\frac{l_2}{2\sin\varphi}} dl\ \left[(l_1 \times l_2) I_1(l;h,\mu) + (l_2 \times l_3) I_2(\varphi,l;h,\mu)\right] \right\}$$

since: $\frac{l_2}{2} = r\sin\varphi_1 \Rightarrow \varphi_1 = \arcsin\left(\frac{l_2}{2r}\right)$

$$\sin\varphi^* = \frac{l_2}{\sqrt{l_1^{\ 2} + l_2^{\ 2}}};$$

and: $I_2(\varphi l;h,\mu) = I_0(h,\mu)\cdot\cos\left(\frac{\pi}{2} - arctg\left(\frac{l}{h}\right)\right)\cos\varphi$

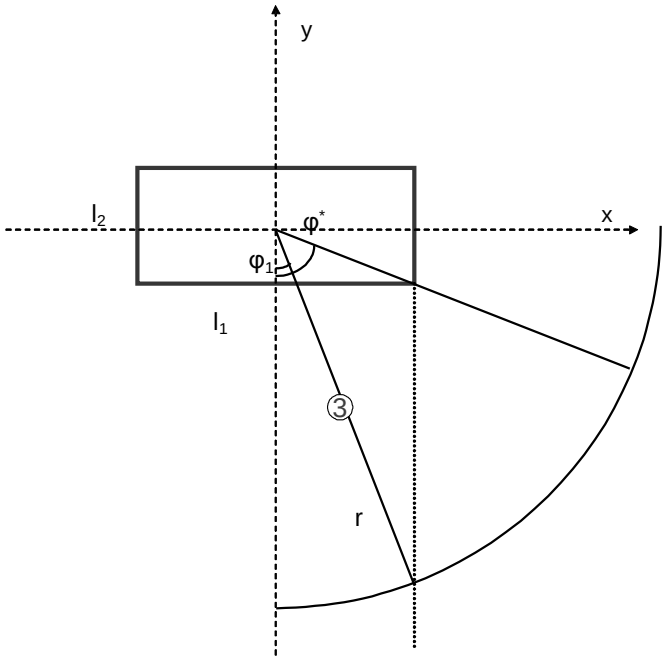

Figure 17. Detector acquisition geometry seen from above (region type 3 is in evidence)

As mentioned the integrand of region type 4 is the same of region type 3 but with the coordinates l_1 and l_2 swapped (see Figure 16) (Figure 18) and the proper interval of integration:

$$N_4 = \frac{\eta C_s}{4\pi}\left\{\int_{\frac{\pi}{2}}^{\frac{\pi}{2}+\arcsin\left(\frac{l_1}{2r}\right)} d\varphi \int_{\frac{l_2}{2\cos\left(\varphi-\frac{\pi}{2}\right)}}^{r} dl \left[(l_1\times l_2)I_1(l;h,\mu)-(l_1\times l_3)I_2\left(\varphi+\frac{\pi}{2},l;h,\mu\right)\right]\right.$$

$$\left. + \int_{\frac{\pi}{2}+\arcsin\left(\frac{l_1}{2r}\right)}^{\frac{\pi}{2}+\arcsin\left(\frac{l_1}{\sqrt{l_1^2+l_2^2}}\right)} d\varphi \int_{\frac{l_2}{2\cos\left(\varphi-\frac{\pi}{2}\right)}}^{\frac{l_1}{2\sin(\varphi)}} dl \left[(l_1\times l_2)I_1(l;h,\mu)-(l_1\times l_3)I_2\left(\varphi+\frac{\pi}{2},l;h,\mu\right)\right]\right\}$$

since is: $l_1 = r\sin\varphi_1 \Rightarrow \varphi_1 = \arcsin\left(\frac{l_1}{2r}\right)$;

and: $\varphi^* + \frac{\pi}{2} = \arcsin\left(\frac{l_1}{\sqrt{l_1^2+l_2^2}}\right) + \frac{\pi}{2}$;

with: $N_4(h) = N_3\left(h; l_1 \to l_2, \varphi \to \varphi' + \frac{\pi}{2}\right)$

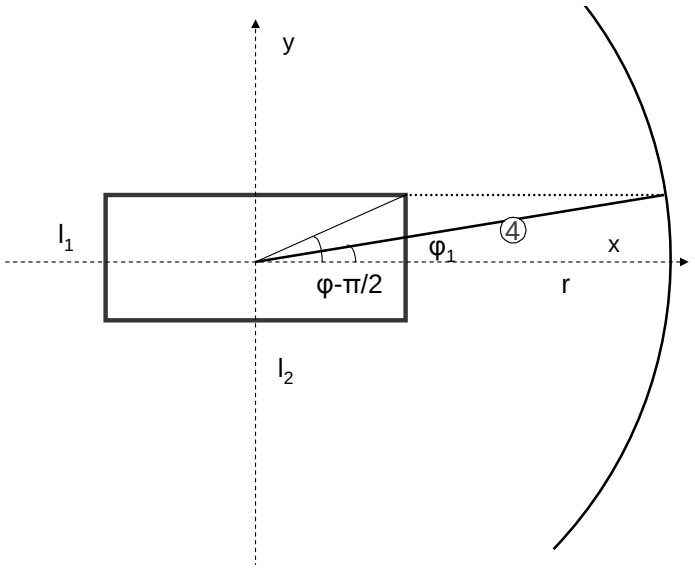

Figure 18. Detector acquisition geometry seen from above (region type 4 is in evidence)

Also for regions of type 3 and 4, the total counts are:

$$N_B(h) = 4 \cdot \left[N_3(h) + N_4(h) \right]$$

Contribution from type 5 and type 6 regions

Regions of type 5 and 6 are almost identical except for the interval of integration in the φ angle. They are defined by:

$$|l_x| \geq \frac{l_2}{2}; |l_y| \geq \frac{l_1}{2};\ |l_x/l_y| < l_1/l_2 \ \text{ and } |l_x/l_y| \geq l_1/l_2$$

In this case the contribution concerning region type 5 will be given by (Figure 19):

$$N_5(h) = \frac{\eta C_s}{4\pi} \int_{\arcsin\left(\frac{l_2}{2r}\right)}^{arctg\left(\frac{l_2}{l_1}\right)} d\varphi \int_{\frac{l_2}{2\sin\varphi}}^{r} dl \left[(l_1 \times l_2) I_1(l; h, \mu) + (l_2 \times l_3) I_2(\varphi, l; h, \mu) - (l_1 \times l_3) I_2\left(\varphi + \frac{\pi}{2}, l; h, \mu\right) \right]$$

while concerning region 6:

$$N_6(h) = \frac{\eta C_s}{4\pi} \int_{\frac{\pi}{2}+\arcsin\left(\frac{l_1}{2r}\right)}^{\frac{\pi}{2}+arctg\left(\frac{l_1}{l_2}\right)} d\varphi \int_{\frac{l_1}{2\sin\left(\varphi-\frac{\pi}{2}\right)}}^{r} dl \left[(l_1 \times l_2) I_1(l; h, \mu) + (l_2 \times l_3) I_2(\varphi, l; h, \mu) - (l_1 \times l_3) I_2\left(\varphi + \frac{\pi}{2}, l; h, \mu\right) \right]$$

as for the previous regions:

$$N_C(h) = 4 \cdot \left[N_5(h) + N_6(h) \right]$$

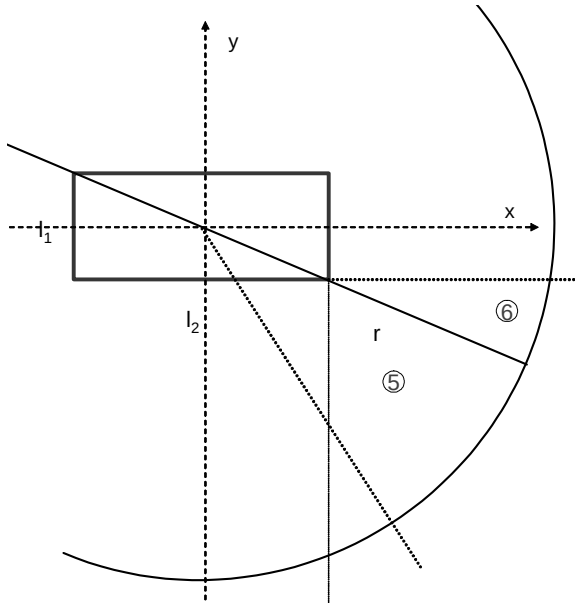

Figure 19. Detector acquisition geometry seen from above (regions type 5 and 6 are in evidence)

Total counts

The contribution of all the regions is:

$$N_{\text{Surface}}^{thick}(h, C_s) = N_A(h, C_s) + N_B(h, C_s) + N_C(h, C_s)$$

Comparison of thin and thick detectors responses

Figure 20 shows the number of counts *vs* the distance at ground (with η= 1 and C_s = 1) for the thin (filled points) and thick (empty box) detectors evaluated above.

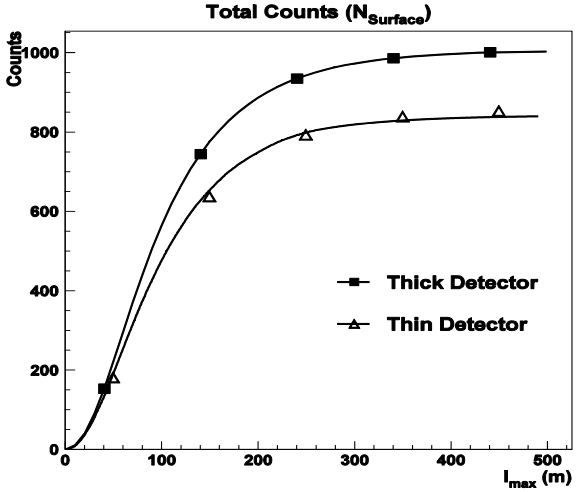

Figure 20. Number of counts *vs* the distance at ground for a thin detector (filled points) and a real thick one (empty box)

It is evident that the thin detector approximation, in the simplified condition, already underestimates the SNIFFER capability of about 20%. On the other hand, in both cases (as pointed out above) the typical on-ground surface that contributes to the counts has a radius of about 300 m.

Air contribution

The typical situation of a nuclear accident when a radioactive plume is released must include both air and ground contaminations (with the reasonable approximation of uniform activities).

The problem can be solved using the considerations of the previous paragraph, integrating on the vertical dimension (allowing the altitude *h* to vary appropriately).

Assuming that $R < h$ and referring to the top hemisphere (volume A, in Figure 21) of the useful spherical volume of the detector one can express the number of counts from that volume (integrating in cylindrical coordinates) as sum of the different contribution coming from the volumes corresponding to the regions defined in the previous section.

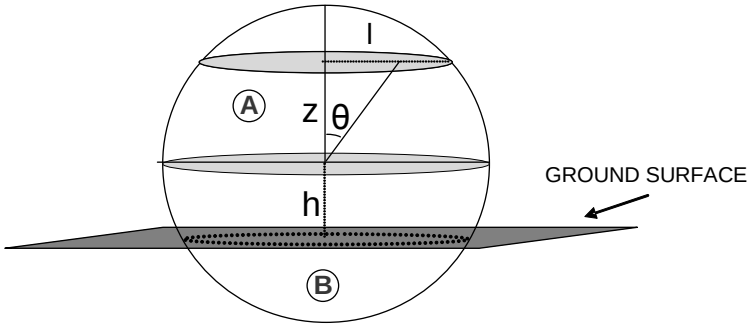

Figure 21. Maximum detectable volume and characteristic parameters in the aerial detection in case of contamination diffused in air. Detector is in the center of the sphere

For the volume of region type 1 the counts are:

$$N_{V1-2}(R) = \int_{\frac{l_3}{2}}^{R} dz \; N_A(z; C_V)$$

where z represents the additional dimension (h in the expressions of the previous section),

C_V) C_V = number of photons per second emitted by the source for cubic centimetre of contaminated area $\left[\frac{photons}{s \cdot cm^3}\right]$;

while for the other regions the integral start from 0:

$$N_{V3-6}(R) = \int_{0}^{R} dz \left[N_B(z; C_V) + N_C(z; C_V)\right]$$

therefore, the total counts of the hemisphere A are:

$$N_{VA}(R) = N_{V1-2}(R) + N_{V3-6}(R)$$

Eventually, the contribution to the counts in the typical situation shown in Figure 21, will come from every emitting infinitesimal element contained in the maximum detectable spherical region to which we will subtract the contribution of those infinitesimal element contained in region B, or in other words:

$$N_{Air}(C_v) = 2 \cdot N_{VA}(R) - N_{VB}$$

where $N_{VB} = N_{VA}(R) - N_{VA}(h)$

h is the aircraft height of flight.

Therefore, if the aircraft devoted to the radiological surveillance flights at an altitude $h < R$ in presence of uniformly diffused contamination in air (C_v) and uniform contamination on ground (C_S), the integral counts of a parallelepiped detector mounted on board of the aircraft will be given by:

$$N = N_{\text{surface}}(C_S) + N_{Air}(C_V)$$

From this equation it seems clear that measures of C_v made directly in plume with the system installed on aircraft would allow the determination of the ground contamination C_S. That constitutes the real innovation with respect to any kind of aircraft, devoted today, to the radiological monitoring activity.

It is worth mentioning that the above analytical derivations require simplifying approximations; however, most of the relevant aspects of the problem are all included. A more detailed approach shall be based on weather science models and finite elements integration (beyond the scope of the present report).

Organic micropollutants in atmosphere: VOC and PAH sampling and analysis

The same aerial platform used for large scale radioactivity survey can be successfully and effectively used to monitor micropollutants in the atmosphere, such as VOCs and PAHs. Concentration of these chemical compounds in air can vary in time and space according to non-uniform distribution of the sources and to different permanence in air, related to chemical and photochemical reactivity of the various molecules.

VOC sampling represents one of the most critical phases of qualitative and quantitative process of air; therefore the sampling system shall guarantee sample representative, to reduce at minimum contaminations and reactions of degradation that lead to formation of compounds with losses of the sampled substances.

There are different VOC sampling methods, we have performed the sampling with Canister, as it is illustrated in the following paragraphs.

Many methods are used to sample and analyze PAH compounds. While particulate matter can be sampled using filters of different materials, PAH compounds in vapour phase can be trapped only if in the sampling line is present an adsorbent material like PUF (PolyUrethane Foam) or XAD-2 resin.

Designing a PAH sampling system: general criteria

In gaseous PAH sampling polyurethane foam filters are used. These filters are penetrated by known air flow. Filters are analyzed in laboratory right after the end of the aerial mission. To perform a correct sampling two parameters shall be kept in mind during the design:

- the air speed penetrating the filters;
- the volume of the sampled air.

In particular, the intercepted air flowing through the filters must have a relative velocity high enough to ensure that filters do not obstruct air flow but sufficiently low to assure the complete deposition of the sample on the filters. Typically automated atmospheric ground based sampling system works with PUF filters having 3 cm of thickness, and it samples air with speed of about 40 cm/s. The SNIFFER system uses filters with 5 cm of thickness to perform sampling also at higher speed.

In relation to the offline analysis, the sampled air volume has to be sufficient in order to extract from the filters enough sample to guarantee a reasonable sensibility of the measuring device. For that reason an overall volume at least equal to the volume (~of 4,000 m^3) sampled in ground station systems must be sampled during the mission.

Particulate characterization for non radiological aspects

The air sample passing a probe and collected on filter, in addition to radioactivity, can also provide information on particulate concentration in sampled air and on sizes of the particles. The former are of fundamental importance for the air quality control, the latter allow to assign different sanitary relevance, according to particles collected, on the basis of different parts of the human respiratory system that can be involved. The greater or smaller ability of a filter to collect particles can be expressed in terms of collection efficiency, either as number of collected particles (E) or collected mass (mass concentration E_m) (11).

Generally the ability of collecting particles for filters can be also defined in terms of its penetration P, that is the fraction of particles that pass the filter respect to the entering ones. Penetration is usually defined as:

$$P = 1 - E_{(m)}\,.$$

Penetration decreases exponentially with increasing filter thickness and it depends on particle size, particle-filter relative speed, filter material solidity and fibre size.

The structure of a filter causes a resistance to air flowing through it (pressure drop). At a given air velocity, the pressure drop in a filter is directly proportional to the thickness of the filter itself.

A wide range of filters of various materials and of different shapes commercially available have different collection characteristics and different collection efficiency. It is important to emphasize that the choice of a certain type of filter is dictated also by the type of analysis that shall be carried out. As an example gravimetric analysis requires that the filter weight is stable with age, changes in temperature and relative humidity. For that reason cellulose fibre filters are quite hygroscopic and generally not suitable for aerosol sampling for gravimetric analysis. Glass fibre and cellulose ester filters are much less affected by moisture and age; polycarbonate, polyvinyl chloride and Teflon filters are affected even less (11).

If the aerosol particles are analyzed by chemical methods, one must be concerned with interferences caused by the filter material or contaminants in the filter. For analytical methods that requires reducing to ashes or dissolving in acid, consideration must be given to the amount and type of filter residue.

The choice of a certain type of filter, therefore, for specific application have to take into account the limits imposed by the mechanical resistance of the filtering material according to the sampling conditions: corrosive characteristics, temperature, humidity.

Teflon filters have been chosen due to their greater mechanical resistance respect to other types of filters and being suitable for gravimetric and morphologic analysis of particulate matter by means of scanning microscopy (11).

Off-line analysis of the collected samples

Once the aerosol sample is collected on filter, the increase in mass of the filter is determined through a weighing of it. This approach requires the ability to weight precisely filters before and after sampling and accurately measure the sampling time. Of course, it need to use filters with low tare weight because the collected particles represent a larger proportion of the total weight and therefore the relative effect of change in filter weight caused by moisture or temperature is negligible.

Typically the scales used in this kind of analysis have to be placed in a room with controlled temperature (±1°C) and humidity (±5% for a relative humidity between 30 and 50%). Indeed in order to minimize the effect of the relative humidity filters have to rest for at least 1 h in the environment before the weighing session.

Static charge can accumulate on filters and cause an error in weighing. It is customary to hold the filter near an alpha radiation source, such as polonium 210, to neutralize the accumulated charge before weighing.

A determination of dimensions of particles collected on filters can be carried out with microscopes. For this scope can be used optical microscopes for particles having diameters 0.3-20 µm, SEM (Scanning Electron Microscopy, resolution 0.01 µm) or TEM (Transmission Electron Microscopy, resolution down to 0.0002 µm) microscopes for smaller particles (11).

SNIFFER SYSTEM: DETAILED IMPLEMENTATIONS

The SNIFFER system is the response to the motivations introduced in chapter 1. Its design and implementation fulfil the system needs discussed in chapter 2.

Mounted on board of the Sky Arrow aircraft (the aerial platform described at the beginning of chapter 2), the SNIFFER permits the radioactive contaminants and air pollution monitoring of large areas in relatively short time.

The system consists of the following components:

- air sampling unit (probe, suction line and filters subsystem);
- radiation measuring unit (BGO, Geiger, HPGe and NaI detectors and relative electronics);
- VOC-PAH sampling unit;
- control and data acquisition subsystem (electronic cards, actuators and sensors).

Table 4 presents the applicable matrix of the functional blocks introduced in the previous chapter and the above components.

Table 4. Functional blocks and implemented components applicable matrix

Units or subsystem	Aerial Platform	Radioactivity contamination measurement	Particulate and injurious gases monitoring
Air sampling			
Subcomponents *Probe, suction line, filter system, needle valve*	X	X	X
Radiation measuring			
Subcomponents *BGO, Geiger, HPGe, NaI and relative electronics*	X	X	
VOC-PAH sampling			
Subcomponents *Sampler, canister*	X		X
Control and Data acquisition subsystem			
Subcomponents *Electronics boards, actuators, sensors*	X	X	X

Since all units are hosted on the aerial platform, they have been chosen taking into account their purposes and trying to:

- minimize the overall dimensions,
- minimize the power consumption (when applicable),
- distribute optimally the weights.

In Table 5 weights and power characteristics of the main system components are reported.

Table 5. Weight and power characteristic of the SNIFFER system

Device	Weight (kg)	Power (V) / (A)
Crate, electronic cards, actuators, Geiger and BGO detector and cabling	*7.5*	24 / 2
Probe (heather)	*0.3*	12 / 4
BGO preamplifier	*1.1*	±12 / 0.5
HPGe detector	*6.6*	12 / 1.1
Multi Channel Analyzer (MCA)	*1.5*	12 / 1.3
VOC-PAH Unit	*10.1*	12 / 3

Air-sampling unit

The sampling unit is located in the front part of the aircraft, which has been properly designed and modified for its correct installation as shown in Figure 22 (see also Figure 25).

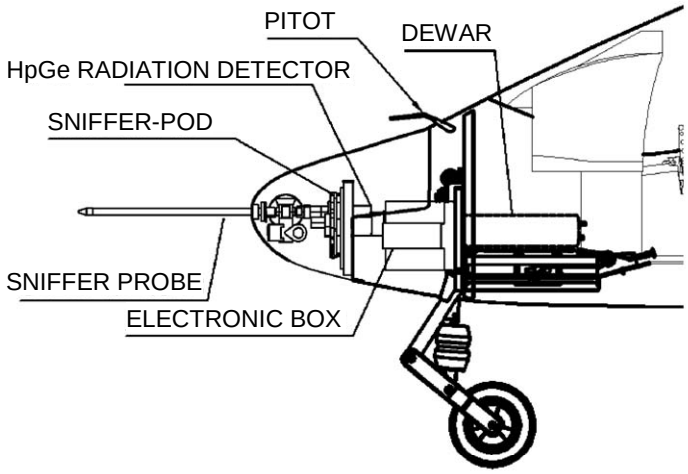

Figure22. Installation of the sampling Unit in the Sky Arrow aircraft

The sampling line is essentially a controlled suction line with filters to collect aerosol samples and radiation detectors; its most important subcomponents are (Figures 23 and 24):

- the probe;
- the Shutter (a controlled valve that opens or shuts the line);
- the sampling filters and the filter-case disk;
- the Holder (a small movable box containing a small BGO detector and a Geiger counter);
- the needle valve that permits to maintain the active isokinetic sampling;
- two radiation detectors (BGO and Geiger).

The sampling probe has to be located where aerodynamic perturbation induced by the advancing of the platform is negligible (see isokinetic condition discussion at page 14).

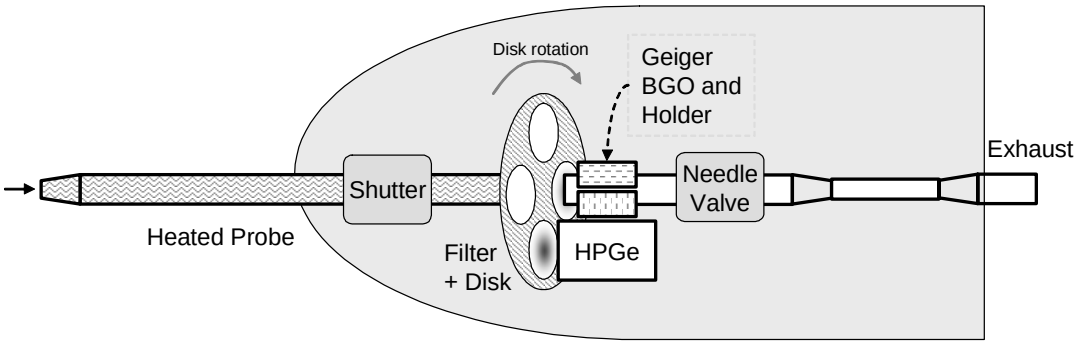

Figure 23. A schematic sampling line

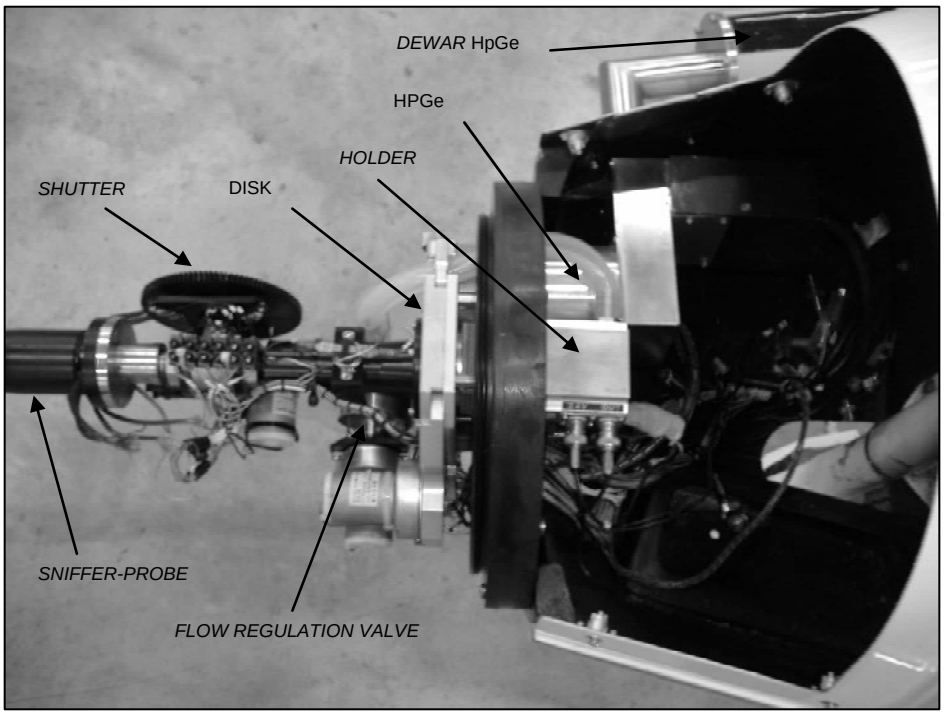

Figure 24. Installation of the sampling Unit in the Sky Arrow aircraft

The probe nose extends ahead by 450 mm and is warmed to prevent air condensation and aerosol deposition along the line, if external temperature in flight goes below the dew point. Resistances are fed from 12 Vdc and manually operated by the pilot.

A diode, installed along the line, is used to measure the nose temperature and monitor the correct operation of the heating bands.

Downstream the suction line a valve (Shutter) determines the aperture of the line itself, while the carrier gas is driven behind the filter and reaches the exhaust line after a Venturi throat.

The filters (up to 4) are housed on an aluminium disk that can rotate around its axis by means of a connected step motor. The exposed filter is determined by the disk rotation and two optical marks assure the correct filter positioning and its identification.

The rotating filter disk is placed downstream the line and has four 47 mm diameter filter holders, one for each of the possible independent aerosol collection during the same flight mission.

During the sampling, the whole line is airtight. On the other hand, in order to permit the disk rotation, the part in contact with it is moved apart a few millimetres before starting the disk movement; this is accomplished by a two steps motor and corresponding optical sensors.

The Holder box guarantees the airtight of the line and contains two small detectors that perform online measurements of gross beta and gamma radioactivity of the aerosol collected on the exposed filter.

The two in-line detectors are: a Geiger counter (external diameter 1 cm) and a small BGO (Bismuth Germanate Oxide) crystal (see detectors description below); both of them are detailed in one of the next sections (see page 35).

Figure 25 shows the front part of the aircraft (see also Figure 24); visible from left to right: the HPGe detector (external dewar and part of the cup behind the filter, discussed later), disk case with Teflon filters (front view), flow regulation valve control and the Shutter (controlled by the black toothed wheel, clearly visible).

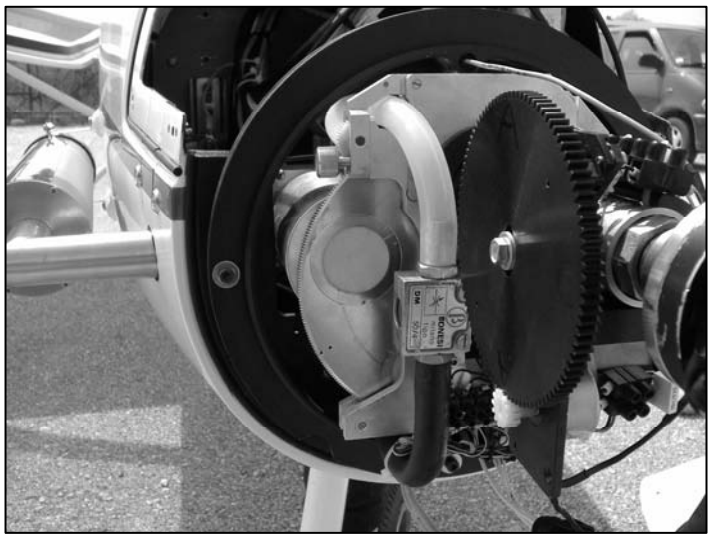

Figure 25. The sampling unit

Active isokinetic sampling of aerosol is reached by continuous automated regulation of a needle valve, aiming to assure a flow speed at the inlet equal to the airplane relative speed (see the isokinetic relation on page 14). The inlet flow scales with aircraft speed and can be regulated within an error of ±1% in the aircraft speed operative range between 30 and 71 l/min for a speed of 80 km/h (~ 43 knots) and 194 km/h (~ 105 knots), respectively.

Environmental and in-flight parameters sensors

The air-transported SNIFFER includes many sensors to measure environmental parameters, that are used in the flow regulation algorithm:

- diodes as temperature sensors;
- pressure transducers to measure pressure and flow velocity indirectly;
- hot wire anemometer to measure air speed into the Sampler duct.

Two diodes allow the determinations of the temperature values used in the flow regulation algorithm. One is located near the nozzle inlet and it measures the external air temperature. The other diode is right after the regulation valve and it provides the temperature of the air flowing into the sampling line at intervals (of several tens of milliseconds) synchronized with the flow regulation action.

A third diode, as previously mentioned, is installed on the probe nose and it provides information about the correct operation of the heating bands.

Pressure data are provided by pressure transducers supplied by DMA-Marchiori of Rome.

An anemometric hot wire sensor (mod. DNE506 produced by LSI, Milano), located into the Sampler duct, acquires at regular intervals information about air velocity inside the duct itself, thus one can deduce air volume sampled by the Sampler.

Finally a GPS receiver provides at prefixed intervals (around 10 seconds) precise information relative to aircraft speed and geoposition. Such information allows the correlation of the acquired data to a space-temporal reference and therefore correctly maps acquired data on a geographical map in a precise temporal extend.

Radiation measuring unit

The radiation measuring unit includes all the detectors that, under the supervision of the acquisition and control system allow the quantitative estimation of the radionuclide activities and the determination of the atmospheric contamination.

The subsystem consists of four detectors.

A small Geiger detector, having 10 mm external diameter, is mounted inside the Holder box (see fig. 26) with the entrance mica window in front of the in-line filter. It is powered by the acquisition and control boards and the generated signals are sent to a pulse counter whose contents is periodically read and stored.

A small in-line gamma detector is made of (1 cm^3) BGO crystal, a photodiode and a signal preamplifier. It is located inside the Holder box, next to the Geiger counter (Figure 26), with the sensible window in front of the filter. It provides online information on the presence of radioactive contaminants on the exposed filter (and therefore on the sampled air) but, due to its very small size, it does not have enough energy resolution to permit the identification of the radioactive isotopes.

A high resolution HPGe (High Purity Germanium) detector allows radionuclide identification in the sample collected on the filters. It has been designed in collaboration with Camberra Semiconductor, taking into accounts the constrains imposed by the SNIFFER and its aerial platform. The system cooling is assured by a dewar filled up of liquid Nitrogen, providing the proper cooling for up to four hours, compatible with the aircraft autonomy. Due to the crystal size, the detector is not inserted into the sampling line, but is located in such manner that with a 90° rotation of the filter disk it can face the last exposed filter. The dewar is flanged to aircraft fuselage but installed externally to it to minimize its influence on penetration efficiency of the aircraft and to facilitate Nitrogen refilling (Figure 27).

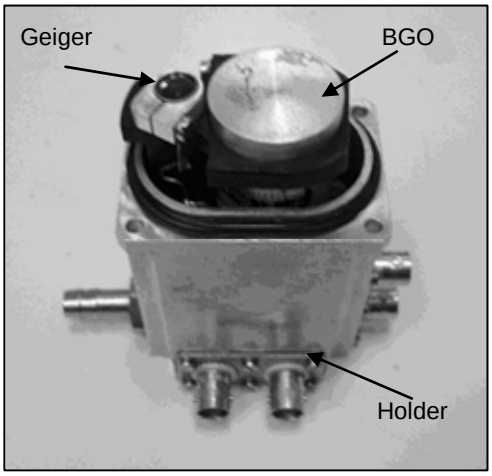

Figure 26. The holder and the hosted Geiger and BGO detectors heads

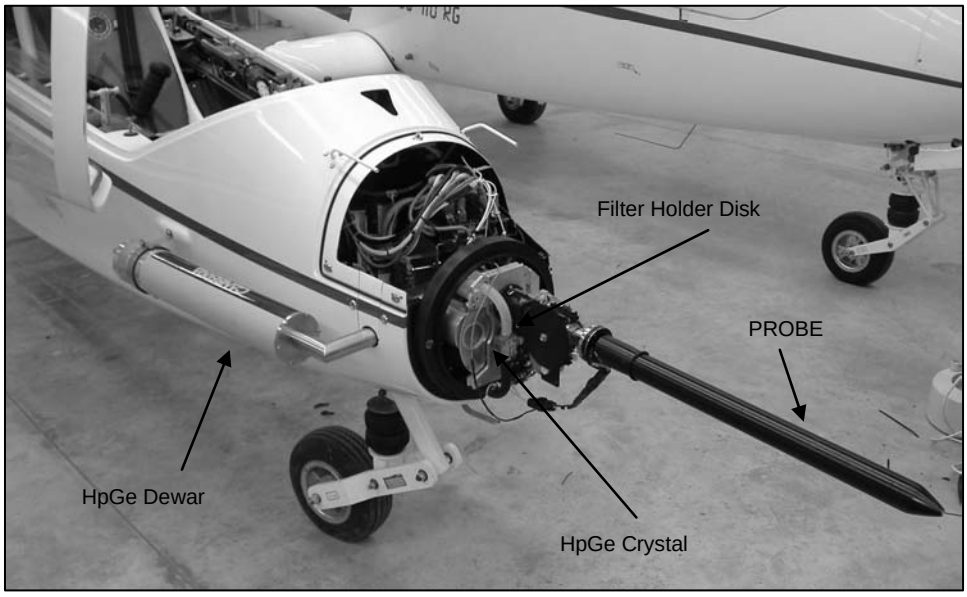

Figure 27. The HPGe dewar on the left and the sampling unit with the long black probe

External to the sampling unit, a high volume NaI(Tl) detector ($400 \times 100 \times 100$ mm^3, 17.5 kg in weight), is installed in the rear part of the aircraft, behind the shoulders of the pilot, in correspondence of an opening hole on the bottom of the fuselage. Figure 28 and Figure 29 shows its installation on board.

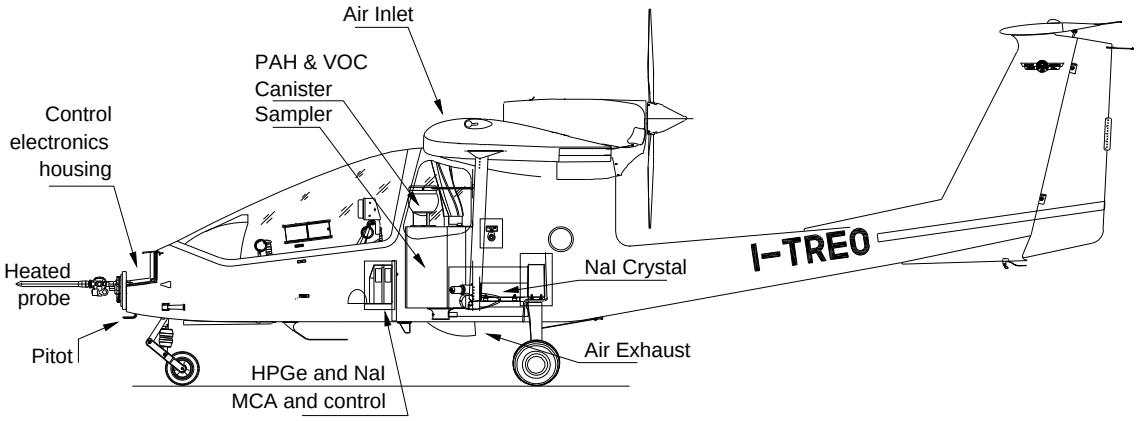

Figure 28. Installation of the SNIFFER in the Sky Arrow

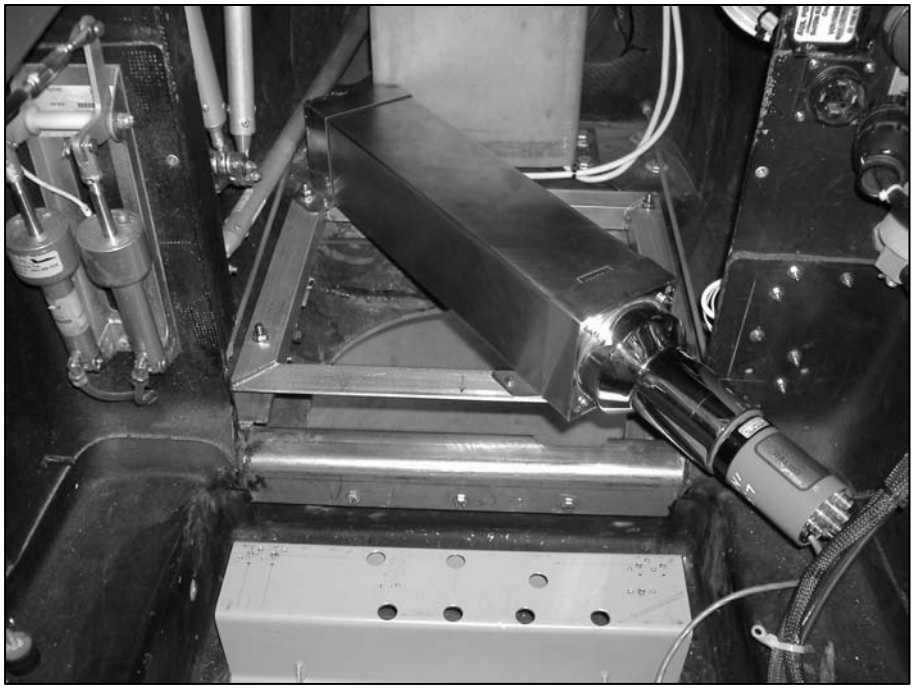

Figure 29. Installation of the NaI detector on the rear part of the Sky Arrow aircraft

The signal from the BGO, the HpGe and the NaI(Tl) detectors are connected to the respective amplifier (and pre-amplifier) and then to the corresponding multichannel analyzer (MCA). Each multichannel device is controlled and acquired via a serial connection. Two

Walklab module produced by Silena S.p.a Milan, (located in the rear part of the aircraft, near the VOC-PAH Unit) control the NaI and HPGe acquisitions and are able to supply high voltages for their correct operability. MCA8000A multichannel (produced by Amptek) controls the BGO acquisition, while its signals are pre-amplified by a NIM module.

Radioactivity measurements

The different detectors have been tested and calibrated, using mainly calibrated sealed sources of ^{60}Co and of ^{137}Cs. These sources have been also located very close to the filter position in the suction line to simulate a contaminated filter.

Each signal coming from the different detectors has been visualized on an oscilloscope and proper actions have been taken to maximize signal to noise ratio.

Moreover, the parameters of each multichannel analyzer (typical spectra are shown in Figures 30-31-32) have been tuned.

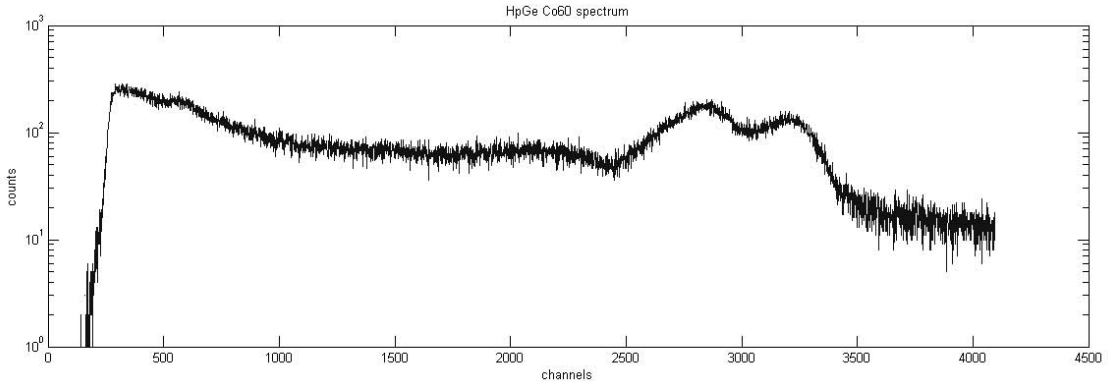

Figure 30. ^{60}Co source spectrum obtained by the NaI detector; the resolution of this detector is enough to identifty quite a few radiactive sources

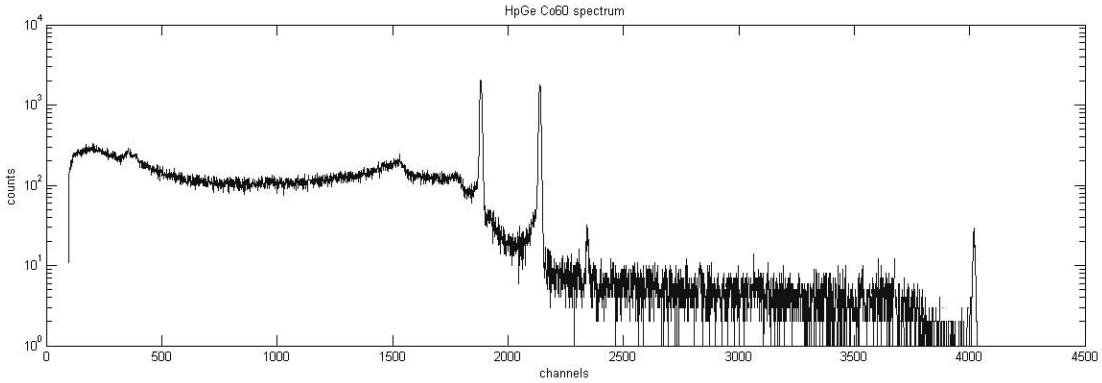

Figure 31. ^{60}Co source spectrum obtained by the high resolution HPGe detector; the high resolution of this device permits the identification of a large number of contaminants

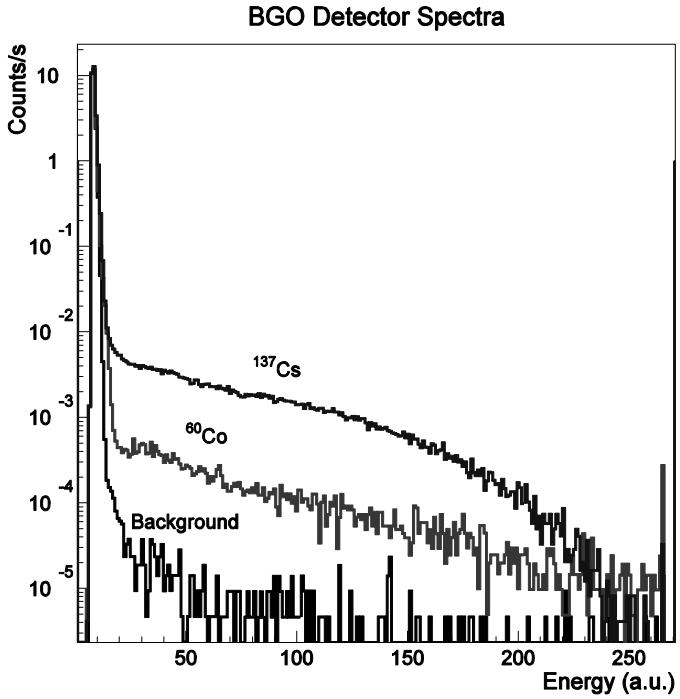

Figure 32. Spectrum obtained using the BGO detector: significant counts above the background (channel 20) is a prompt evidence of presence of activity in the filter sampled aerosol

VOC-PAH sampling unit

The VOC-PAH sampling unit (Figure 33) is located in the rear part of the aircraft, behind the pilot (see Figure 28). It is made by two sub-units:

– the canister that performs VOC sampling;
– the Sampler, specifically designed for PAH sampling.

In order to minimize space occupancy, the canister is installed on top of the Sampler as show in Figures 33. The canister is made of a 6 litres spherical stainless-steel reservoir and a throttle valve that allows the suction of the air samples. When the valve is open, the air fills the canister (where a relatively high vacuum has been previously produced) through a line that picks up inside the Sampler before that air penetrates filters mounted on its side walls. A flow limiter conditions the inlet flow and therefore the sampling length of the canister.

The Sampler is a cave cylinder modelled to convey the air on the internal filters (Figure 34). It is equipped with an exhaust throttle valve installed on the bottom part.

The Sampler samples PAH by means of three PUF (PolyUrethane Foam) filters. Each filter is arranged into the conveyor, which is equipped of baffles to intercept air and let its flow to penetrate filters in radial direction. Air enters the Sampler from an aircraft inlet located in the upper part of the fuselage and is canalized to reach filters. The pilot can control the opening and the shuttering by means of an appropriate switch. The air that passed the filters reaches the exhaust valve and is released back into the atmosphere.

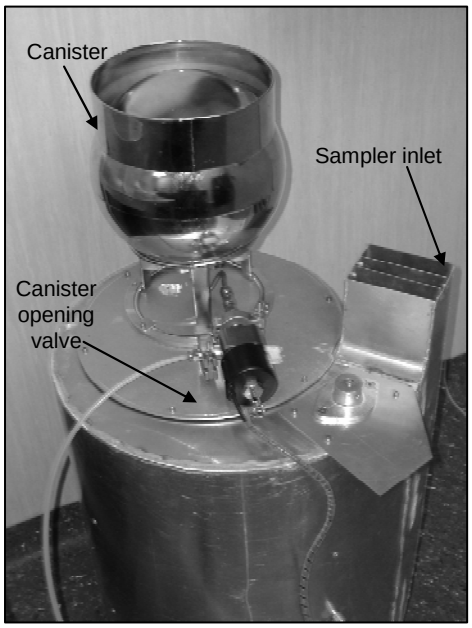

Figure 33. Sampler and canister

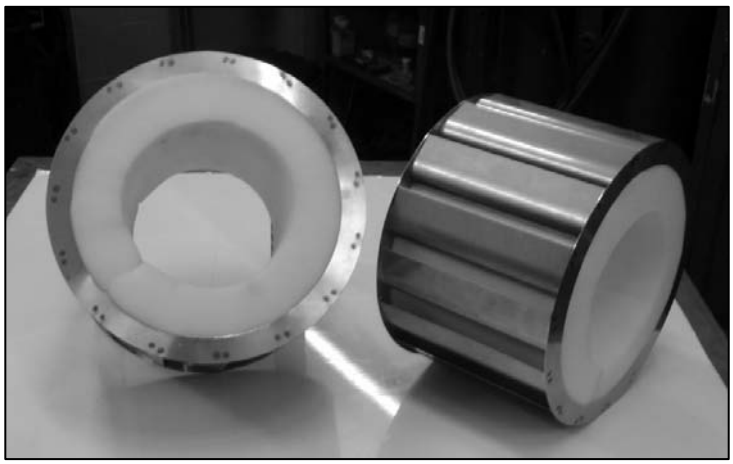

Figure 34. The Sampler conveyors and the PUF

The PAH Sampler implementation

The PAH Sampler is a specially designed system for PAH sampling in air having characteristic features that take into account air speed at the filter inlets and air volume sampled. On the basis of structural characteristic of Sampler, it is possible to calculate easily the aircraft speed that allows, in the span of time devoted to mission, the collection of samples useful for laboratory analysis.

The design of the PAH sampler must comply with the following criteria:

a) reduction of the flow velocity from the aircraft speed at the entrance of the VOC-PAH sampling line to the typical velocity of the PAH sampling system at ground at which the conventional sampling methodology has been tested;
b) maximizing the sampled volume within the typical time of a mission (SKY Arrow endurance: 4 hours);
c) minimizing friction effects in the duct derived by abrupt direction variations, shear stress due to transverse velocity gradient and turbulence;
d) conveying the streamlines to impact the PUF filters at the angle of 90 degrees.

The above criteria have been fulfilled taking into account the following considerations and implementation details:

– *Criterion a)*
The aircraft speed, and then the speed of the inlet sampled air, can be varied from about 43 knots (≈80 km/h = 2.2 10^3 cm/s) to about 105 knots (≈195 km/h = 5.4 10^3 cm/s). In the on ground sampling units, air flow impacts the PUF filter, whose thickness is 3 cm, at about 40 cm/s; in these conditions tests have been performed to guarantee that PAH is well adsorbed in the PUF filter. A substantial increase of the section of the flow between the entrance and the filter surface must then be performed. Due to the aircraft space constraints, the only way to increase the section is adopting a circular geometry for the filters and then to perform, by the mechanical construction of the duct, a change from an horizontal geometry at the inlet to a circular geometry at filters. In the SNIFFER, the inlet cross section is S_1 = 11x7 = 77 cm^2, while the cross section at the level of the anemometer (that permit the measure of the sampled flow) is S_2 = 20x11x3 = 660 cm^2 and the total impact surface of the three filter stack is S_3 = 20x78x3= 4680 cm^2; therefore, the corresponding airflow speed reduces by a factor of 8.6 from entrance to anemometer, and by a factor of 60 at the filter impact, as detailed in Table 6. The thickness of the adopted filter is 5 cm to take into account the possible larger speed of the flow at the filter surface respect to the protocol used in the ground based sampling units. Values shown in Table 6 do not take into account the impedence of the duct and of the filter that certainly reduces the airflow velocity. The real airflow speed is measured by the anemometer along the sampling line.

Table 6. Sampled volume at different aircraft velocity compared to a typical ground based sampling station

Sampling type	Air speed				Air Flow	Sampled volume	Sampling Time
	inlet		*anemometer*	*filter surface*			
	(km/h)	*(cm/s)*	*(m/s)*	*(cm/s)*	*(m^3/h)*	*(m^3)*	*(h)*
Aircraft							
minimum speed *(43 knots)*	80	2.2 10^3	2.56	36.7	618	2470	4
low operative speed *(60 knots)*	111	3.1 10^3	3.6	51.7	870	3480	4
high operative speed *(90 knots)*	167	4.6 10^3	5.4	76.7	1290	5170	4
maximum speed *(105 knots)*	195	5.4 10^3	6.28	90	1515	6065	4
Ground based station				40	56.7	1360	24

– *Criterion b)*
According to Table 6, the typical volume sampled by the PAH ground station is around 1360 m^3 obtained by a sampling system having a PUF filter surface of 17.5x22.5 ≈ 394 cm^2 with a flow having a speed of 40 cm/s and a sampling time of 24 hours. While the speed of the flow at the filter surface is larger (up to a factor of about 2) than ground based system, the aerial platform is able to sample a much larger volume in about 1/6 of the ground sampling time. The impedence of the duct (not accounted in Table 6) will reduce the sampled volume, that is derived by the anemometer measured speed, knowing the cross section of the duct in front of it.

– *Criterion c)*
To avoid turbulence the sampler design must favour a streamline steady flow with very small impedance (friction). The flow, due to the low velocity, is also incompressible. This is a regime in which the above mentioned Daniel Bernoulli's theorem is applicable. The design of the sampler shape shall keep uniform the streamline flow characteristic of the aircraft motion along the sampling line, taking into account the validity of the Bernoulli equation. A bidimensional flow, as a good approximation for one case, is assumed for simplicity.
For an incompressible steady flow, for each streamline, in every point holds:

$$p + \frac{1}{2}\rho v^2 = \text{constant}$$

Being the motion of streamlines, before entering the sampling line (aircraft velocity field), uniform, then with velocity circulation zero, and being also inviscid (very low friction) and incompressible, Lord Kelvin's theorem guarantees that the velocity circulation remains constant, (zero in the specific case), for the flow along the duct. Stokes' theorem relates the velocity circulation along a closed line to the integral of the rotor velocity across the surface defined by the closed line (still zero). This result holds for arbitrary closed lines enveloping arbitrary small areas and then the rotor velocity is everywhere zero; in other worlds, the flow is irrotational.
It can be shown that the combination of the irrotational flow condition and of the validity of the Bernoulli equation makes the constant in the Bernoulli equation the same for all the streamlines, everywhere in the flow.
Considering the flow in the circular geometry duct and differentiating the Bernoulli equation along the radial direction respect to a generic streamline, we have:

$$\frac{\partial p}{\partial r} + \rho v \frac{\partial v}{\partial r} = 0$$

The radial equilibrium of a streamline is due to the balance of the two main forces acting on it, the pressure gradient and the centripetal force:

$$\frac{\partial p}{\partial r} = \rho \frac{v^2}{r}$$

From the last two equations:

$$\frac{v}{r} + \frac{\partial v}{\partial r} = 0 \text{ that is } \frac{\partial v}{v} = -\frac{\partial r}{r}$$

and then:

$$\ln v = -\ln r + \text{const},$$

that is $$v = \frac{const}{r}$$

This is the relation that the mechanical design of the duct shall favour in order that the streamlines (representing in a steady flow the actual motion of the fluid particles) can be conveyed without disturbance to the filter.

As previously written, in order to decrease the airflow velocity at the filter surface to values compatible with the practice used on ground sampling stations, the geometry chosen for the filters is circular and more precisely they are deployed at the surface of a cylinder. In order to have a flow uniformly distributed along an horizontal section of the cylinder, the streamlines must impact the circumference, where the filter is located, at a constant angle independently on the azimuthal angle, i.e. the radial component of the velocity must be constant all along the circumference.

This means that the angle between the tangent to the circumference and the streamlines must be constant everywhere along the circumference. This should also be valid for any radius of the circumference.

All these requirements are satisfied if the streamlines follow a line defined by the logarithmic spiral curve:

$$r = ae^{b\phi}$$

where r (radial) and ϕ (azimuthal) are the bidimensional polar coordinates, *a* is a scale constant and and *b* is defined by the constant angle (α) between the tangent to the curve in a point and the line connecting that point to the origin of the curve: $b = cot\ \alpha$.

All the streamlines have the same value of α (then of *b*), constrained by the mechanical structure, but different values of *a*.

Then the chosen mechanical design of the sampler follows a Jakob Bernoulli (logarithmic) spiral curve, as shown in Figure 35.

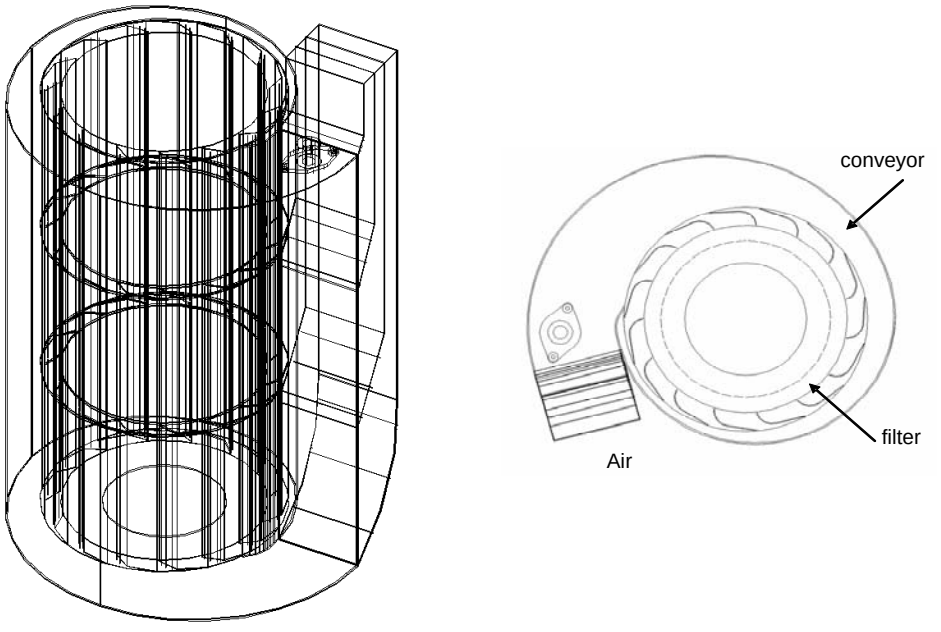

Figure 35. AUTOCAD 3D and top views of the PAH Sampler

– *Criterion d)*
The impact angle of the streamlines with the filter (often called the pitch angle, the complement of α angle), that follows the shape of the chosen logarithmic spiral curve should have been 14° degrees. A system of multiple conveyors (see Figure 35) increases the impact angle to 90° degrees. The conveyors are attached to the cylinder holding the PUF filters. In this way the impact angle is equal to the angle used by the ground based sampling stations avoiding possible differences connected to the geometry of the inner structure of the polyurethane foam.

Control and data acquisition subsystem

A management unit is dedicated to the control of the devices of the SNIFFER (detectors, sensor and transducers) and to the acquisition of signals coming from them.

This sub-system is made of:

1. two 386-compatible CPU boards (Mesa 4C60 and Mesa 4C28) (12) in PC104 and PC104 Plus standard. The two boards communicate by the respective parallel ports (laplink protocol) in a master-slave scheme. The use of the PC104 offers a reliable operation in a very compact solution, fitting the strong constraints on the available room for the electronics;
2. a PC104 card equipped with a series of Digital to Analog Converters (DAC DM121 produced by DMA-Marchiori of Rome) to handle the flow regulation valve;
3. a standard PC104 card (Mesa 4I22) (12) to manage the digital TTL input/output signals of the Shutter, Holder, filter Disk, Canister and Sampler sensors and to drive the regulation of the Geiger high voltage;
4. a custom board consisting mainly of voltage regulators to provide the proper power supplies to several devices;
5. a custom board for signal conversion (sensor specific to TTL and vice versa).

A logical overview of the different devices and how they are connected is presented in Figure 36.

The Mesa 4C60 board acts as master in the 4C60-4C28 communication. It is equipped with a SVGA video card used to visualize messages (for the operator/pilot) on a 9” colour screen. The board is also connected to a 3 keys keyboard to allow the main operations on the system: start/stop of the acquisition, and filter change. The Mesa 4C60 is provided with two (RS232 16C550) serial ports connected to the GPS device and to the NaI(Tl) Walklab.

The Mesa 4C28 board, the DM121 and the Mesa 4I22 cards are directly connected to the 4C28 104 connector. The 4C28 has two serial ports connected to the HpGe Walklab and the BGO MCA8000A device. Finally, the 4C28 is provided with eight inputs ADC[3] for temperature and pressure data acquisition from sensors installed on aircraft. At bootstrap two different applications run on the two CPU boards. Each application read its own configuration file (text format) that contains all relevant parameters that can be optimized during the mission planning. The two applications communicate (asynchronously) by means of messages transmitted on parallel port; in order to guarantee high reliability, the message passing protocol is very simple and minimalist.

[3] The choice of two different CPU boards is due to: the original need of two active controllers in two parts of the aircraft; the need of a VGA interface (absent in the 4C28) and an ADC chip (not available on the 4C60).

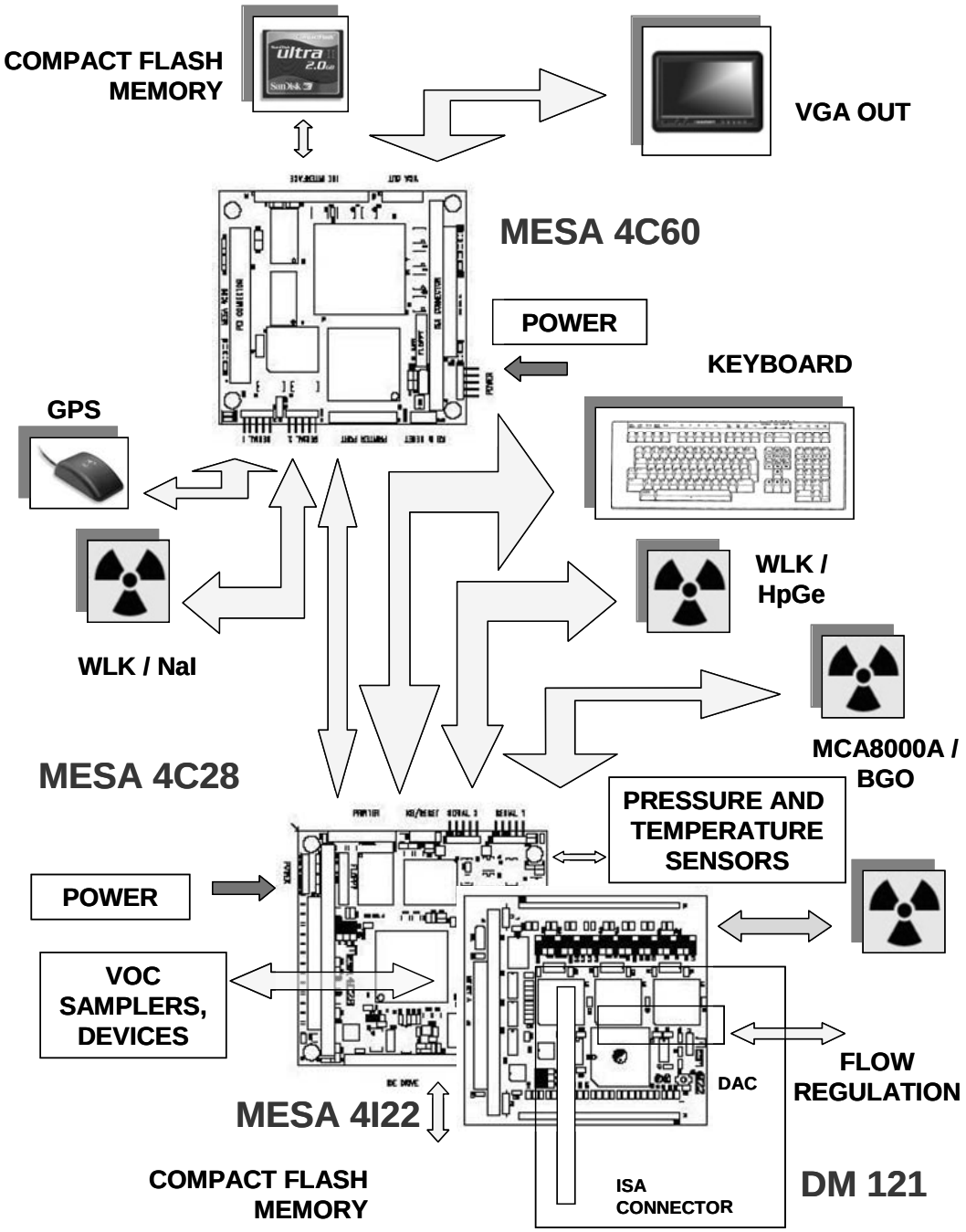

Figure 36. Control and data acquisition components and connection scheme

Generally, the slave sends all status messages to the master that provides their visualization on the small screen. Both applications save logging messages on specific files.

The application flow-charts and their interactions are represented in Figure 37.

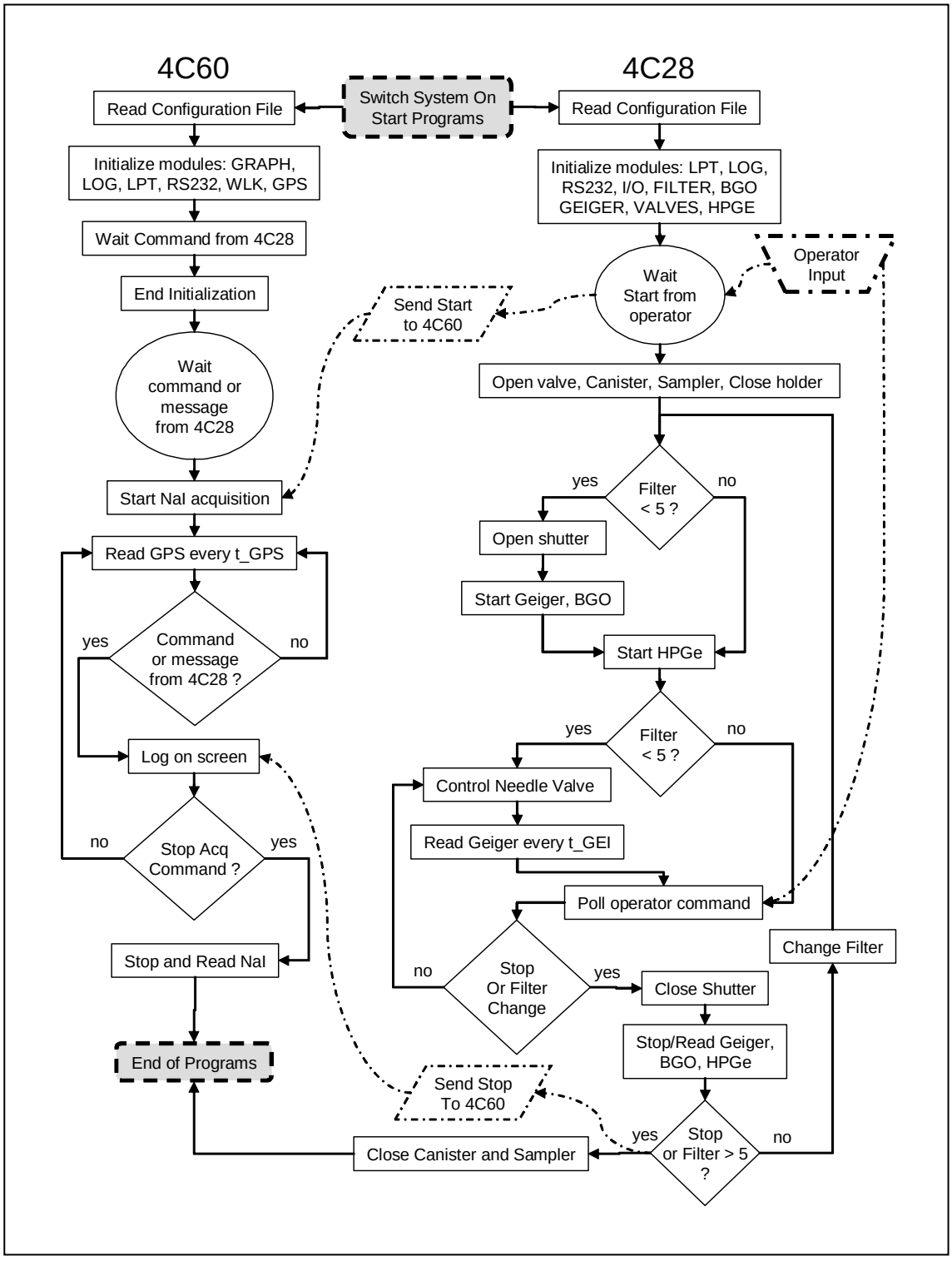

Figure 37. Control and data acquisition software flow chart

The initialization and final phases are serialized on the two CPUs. Main control is delegated to the 4C60. During the acquisition the 4C60 receives messages from the 4C28 and handle the commands from operator by means of the 3 keys keyboard. Periodically it reads GPS stream data and store them on the on-board flash card.

On the other hand, the 4C28 is responsible of the regulation of the flow (via the regulation valve) in order to keep the isokinetic conditions and periodically reads the Geiger's counter. Besides it stops the acquisitions, read data acquired and save them on files at fixed times (defined during the mission plan); eventually it changes the filter (by operator action or at planned intervals).

The operator screen (Figure 38) connected to the 4C60 VGA interface is virtually split into two windows: the upper one displays information about the status of the devices; on the lower window scrolling log messages are shown. The verbosity of the visualized messages can be controlled at configuration time.

Acquired and processed data (from GPS sensor as well), and all information about the status of the system are saved on files in two fast flash cards connected to the two CPU boards.

Figure 38. SNIFFER system operator screen
(SHU = Shutter, HOL = Holder, FIL = Filter, VAL = valve, NaI, HpG, BGO indicate relative detectors, while GEI = Geiger, PRE = pressure sensors, CAN = canister, SAM = Sampler and TEM = temperature sensors. DI/O indicates the communication status between 4C28 and 4C60 cards)

STATUS OF THE PROJECT AND FUTURE PLANS

All the instrumentation has been installed on a customized Sky Arrow airplane. The whole system (modified fuselage, external HPGe dewar and board instrumentation) has got the authorization to flight in the Italian territory, fulfilling the severe criteria of the Italian Airworthiness Authority.

Test flights are in progress to commission and calibrate the various components. During these tests, the SNIFFER is performing quite in agreement to the design specifications.

Operative test flight missions are expected to start soon.

Future developments of the SNIFFER concern at least 4 aspects: increase the number of sampling filters (the current system is limited to 4); install the proper sensors for meteorological parameters that will be exploited by the forecasting models; upgrade the control and acquisition system electronics and software; provide an up/down link to a ground based control room for real-time data analysis and mission reschedule; move toward an unmanned aerial platform.

In the following sections all these planned upgrades will be very shortly discussed:

– *New electronics and software*
  The present control system hardware is based on about 15-year-old design and most of its sub-components are obsolete or can be replaced by highly integrated boards. Moreover, the new boards will integrate modern high speed interfaces (such as USB) that will be connected to new, compact and powerful multichannel analyzer. This hardware upgrade will go in parallel to the upgrade of the software and its porting to the C language and to a real-time Linux based platform, where the drivers of the new electronics devices are available.

– *Additional sensors for meteorological parameters retrieval*
  The estimation of the on-ground and air contaminations and the forecast of their development generally require complex simulation and modelling, as mentioned in chapter 2. These models are based on meteorological parameters acquired by a grid of meteorological ground stations. The sampling of the meteorological conditions by the SNIFFER (time correlated to the radiological data and the ground base information) is expected to have a positive impact in the plume forecasting. A quantitative analysis of such improvement will be carried on in the coming months and the identified sensors will possibly be integrated in the upgraded SNIFFER.

– *New filter subsystem*
  The SNIFFER has a disk hosting a maximum of 4 filters for air sampling along the suction line. A new joke box like filter holder and sequential distributor is under definition. It will store 15 or more filters. The cross contamination between them is avoided by the use of two cylindrical containers (for empty and sampled filters). A small mechanical device will get a new blank filter from the corresponding cylinder and move into the suction line for sampling. At the end of the sampling interval the filter is moved in proximity of the HPGe detector head and from there stored in the sampled filter cylinder. In this way, the SNIFFER will allow a larger number of exposures and therefore shorter sampling geographical paths.

– *Communication operability between the aircraft and a ground emergency Operations Centre*
  The current SNIFFER has a minimum interface with the operator (the aircraft pilot) and all the acquired data is stored on local memory cards. The data is therefore processed at

the end of the flight mission. A major improvement of the SNIFFER is the ability to transmit the acquired data (and be controlled) in real time to (from) a ground-based control room. The current system does need a modest data bandwidth of the order of 350 bytes/s (downlink) and few bytes/s (uplink). This narrow band is currently available in at least two quite different technologies: the radio transmission (VHS at 450 MHz) and the satellite communication (such as Globalstar). The satellite transmission guarantees a large scale coverage but must rely on a private company which will route the data into Internet. On the other hand the VHS radio communication needs line-of-sight between the antennas and therefore, a second airplane, operating as transponder, may be required in case of rather inaccessible area (with complex orography).
In both solutions, the data will reach the Operations Centre control room via a standard Internet connection.

– *Unmanned aircraft*
A real-time up/down link of the SNIFFER is a cogent requirement for a major upgrade of the aerial platform.
Since the beginning of the project one objective was that the instrumentation should be, for weight and power consumption requirements, also compatible with its use on an unmanned aircraft (UAV). In emergency near field operations, near the plume release point, the level of in-plume radiation could be un-compatible with a monitor system operated by a man, whatever his function could be.
UAV, moreover, can be managed in flight without any piloting skill, thus allowing system operations also to scientists and engineers more familiar with payload issues instead than aeronautics. Other advantages would derive from the possibility to perform automatic flight, which can be planned using user friendly graphical tools and a continuous position and altitude above ground control. Different flight patterns that maximize sampling efficiency can be prepared and executed. During automatic flight the operator can always resume UAV control in order to perform an unplanned and detailed sampling of suspect areas. It is worth mentioning that UAV are now becoming common tools in military and civil protection operations and at present national and international regulations are being modified in view of a more spread utilization utilisation of such vehicles.

Detailed results of the tests and calibration as well as performance during the operative missions will be presented in a future document.

REFERENCES

1. United Nations Scientific Committee on the effects of Atomic Radiation. Annex J: Exposures and effects of the Chernobyl accident. In: *UNSCEAR 2000 REPORT Vol. II Sources and effects of ionizing radiation*. Available from: http://www.unscear.org/docs/reports/annexj.pdf; last visited 16/1/2007.
2. Chernobyl: Assessment of radiological and health impacts. *NEA Report*, 2002. Available from: http://www.nea.fr/html/rp/reports/2003/nea3508-chernobyl.pdf; last visited 16/1/2007.
3. United Nations Scientific Committee on the effects of Atomic Radiation. Annex D: Exposure from the Chernobyl Accident. In: *UNSCEAR 1988 REPORT Vol. II Sources and effects of ionizing radiation*. Available from: http://www.unscear.org/pdffiles/1988annexd.pdf; last visited 16/1/2007.
4. *Atlas of Chernobyl deposition in Europe after the Chernobyl accident*. Luxembourg: EC Office of Publication; 1996. (EUR Report 16733).
5. Bertocchi A, Crateri R, Frullani S, Gaddini M, Garibaldi F, Giuliani F, Gricia M, Maselli R, Monteleone G, Mazzini F, Naddeo C, Saluset B, Santavenere F, Tacconi O, Vischetti M. Remote sensing of fission products gamma rays radioactive contamination. *Physics in Environmental and Biomedical Research* 1986;361-6.
6. Il rischio ambientale nella produzione di energia: risultati sperimentali, calcoli e riflessioni dopo Chernobyl. *Annali dell'Istituto Superiore di Sanità* 1987;23(2).
7. Italia. Decreto legislativo n. 171 del 21 maggio 2004. Attuazione della direttiva 2001/81/CE relativa ai limiti nazionali di emissione di alcuni inquinanti atmosferici. *Gazzetta Ufficiale* n. 165 del 16 luglio 2004.
8. European Union. Corrigendum to Regulation (EC) No 850/2004 of the European Parliament and of the Council of 29 April 2004 on persistent organic pollutants and amending Directive 79/117/EEC (Official Journal of the European Union L 158 of 30 April 2004). *Official Journal of the European Union* L 229/5 29/6/2004. Available at: http://eur-lex.europa.eu/LexUriServ/site/en/oj/2004/l_229/l_22920040629en00050022.pdf; last visited 23/5/07.
9. European Union. Regulation (EC) No 166/2006 of the European Parliament and of the Council of 18 January 2006 concerning the establishment of a European pollutant release and transfer register and amending Council Directives 91/689/EEC and 96/61/EC. *Official Journal of the European Union* L 33/1 4/2/2006. Available at http://eur-lex.europa.eu/LexUriServ/site/en/oj/2006/l_033/l_03320060204en00010017.pdf; last visited 23/5/07.
10. Rindone B, Beltrame P, De Cesaris AL. *Il benzene e altri composti aromatici: monitoraggio e rischi per l'uomo*. Milano: Fondazione Lombardia per l'Ambiente; 1998.
11. Hinds WC. *Aerosol technology: properties, behavior, and measurement of airborne particles*. New York: John Wiley & Sons; 1982.
12. Mesa Electronics. MESA PC/104 CPU Information. [web page]. Richmond, CA: Mesa Electronics. Available from http//www.mesanet.com; last visited 7/11/2007.

Other documents

Castelluccio DM. Allestimento di un velivolo ultraleggero strumentato per rilevamenti ambientali. [Thesis]. Rome: Università degli Studi "La Sapienza"; 2005.

Castelluccio DM, Chiavarini S, Cisbani E, Del Prato U, Fracasso G, Fratoni R, Frullani S, Gaddini M, Giuliani F, Marchiori G, Mostarda A, Paoloni G, Pianese E, Pierangeli L, Sbuelz A, Siciliano G, Veneroni P. Aerial platform for in-plume sampling and on-line measurements in the emergency early

phase. In: *Proceedings of International Conference on Monitoring, assessment and uncertainties for nuclear and radiological emergency response*; Rio de Janeiro (Brazil), November 21-25, 2005.

Castelluccio DM, Chiavarini S, Cisbani E, Del Prato U, Fracasso G, Fratoni R, Frullani S, Gaddini M, Giuliani F, Marchiori G, Mostarda A, Paoloni G, Pianese E, Pierangeli L, Sbuelz A, Siciliano G, Veneroni P. A Chernobyl lesson for aerial monitoring: integration of passive measurements with active sampling in the emergency early phase. In: *Proceedings of IRPA Europe2006* (poster session). Paris (France), May 15-19, 2006.

Castelluccio DM, Chiavarini S, Cisbani E, Colangeli G, Del Prato U, Fratoni R, Frullani S, Fuselli S, Gaddini M, Giuliani F, Marchiori G, Marconi A, Mostarda A, Paoletti L, Paoloni G, Pianese E, Pierangeli L, Veneroni P, Viviano G. Una piattaforma strumentata per studi della qualità dell'aria e monitoraggio ambientale anche in condizioni di incidente radiologico. In: *Atti del Congresso Nazionale della Società Italiana di Fisica*. Torino 18-23 settembre, 2006. p. 44

Castelluccio DM, Chiavarini S, Cisbani E, Del Prato U, Fratoni R, Frullani S, Gaddini M, Giuliani F, Marchiori G, Mostarda A, Paoloni G, Pianese E, Pierangeli L, Veneroni P. Piattaforma aerea strumentata per campionamento e misure di radioattività per monitoraggio ed interventi in diverse situazioni incidentali. In: *Atti del Congresso Nazionale di Radioprotezione, organizzato da AIRP (Associazione Nazionale di Radioprotezione*); Torino, 20-23 settembre, 2006. p. 37.

Stampato da Litografia Chicca di Fausto Chicca
Via di Villa Braschi 143, 00019 Tivoli (Roma)

Roma, settembre 2007 (n. 3) 18° Suppl.